Resolved X-ray Line Profiles from O Stars as a Diagnostic of Wind Mass Loss

David Cohen
Department of Physics & Astronomy
Swarthmore College

Jon Sundqvist (Delaware and Munich), Maurice Leutenegger (GSFC), Stan Owocki & Dylan Kee (Delaware), Véronique Petit (Florida Institute of Technology), Marc Gagné (West Chester), Asif ud-Doula (Penn St. Worthington-Scranton)
with
Emma Wollman (Caltech, Swarthmore ’09), James MacArthur (Stanford, Swarthmore ’11), Zack Li (Swarthmore ’16)

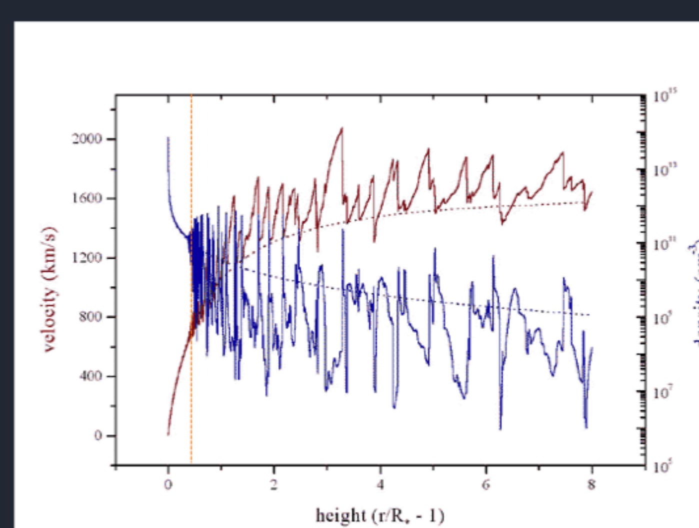

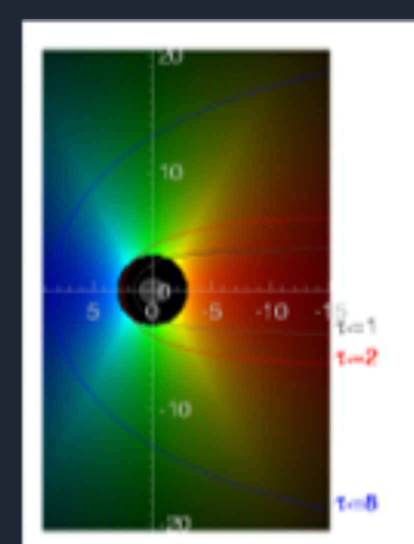

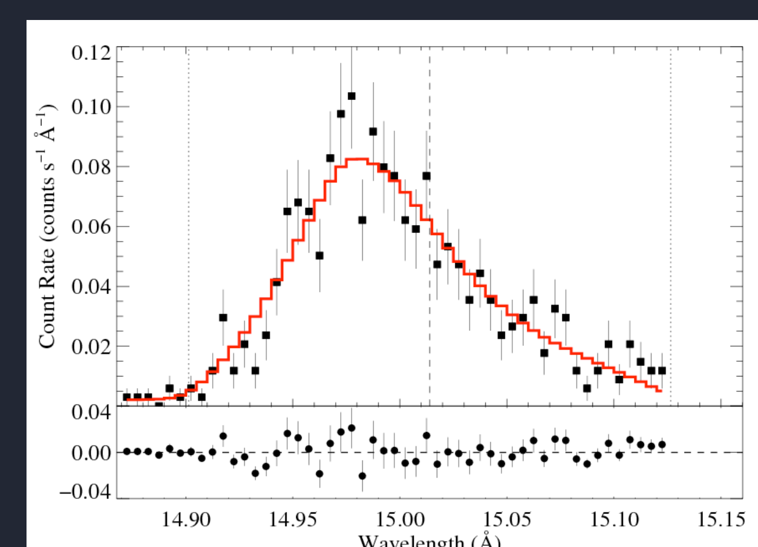

Soft-X-ray emission is ubiquitous in O stars

$L_X \sim 10^{-7} L_{Bol}$ ($L_X \sim 10^{31}$ to 10^{33} ergs s^{-1})

soft thermal spectrum, kT ~ few 0.1 keV

minimal time variability

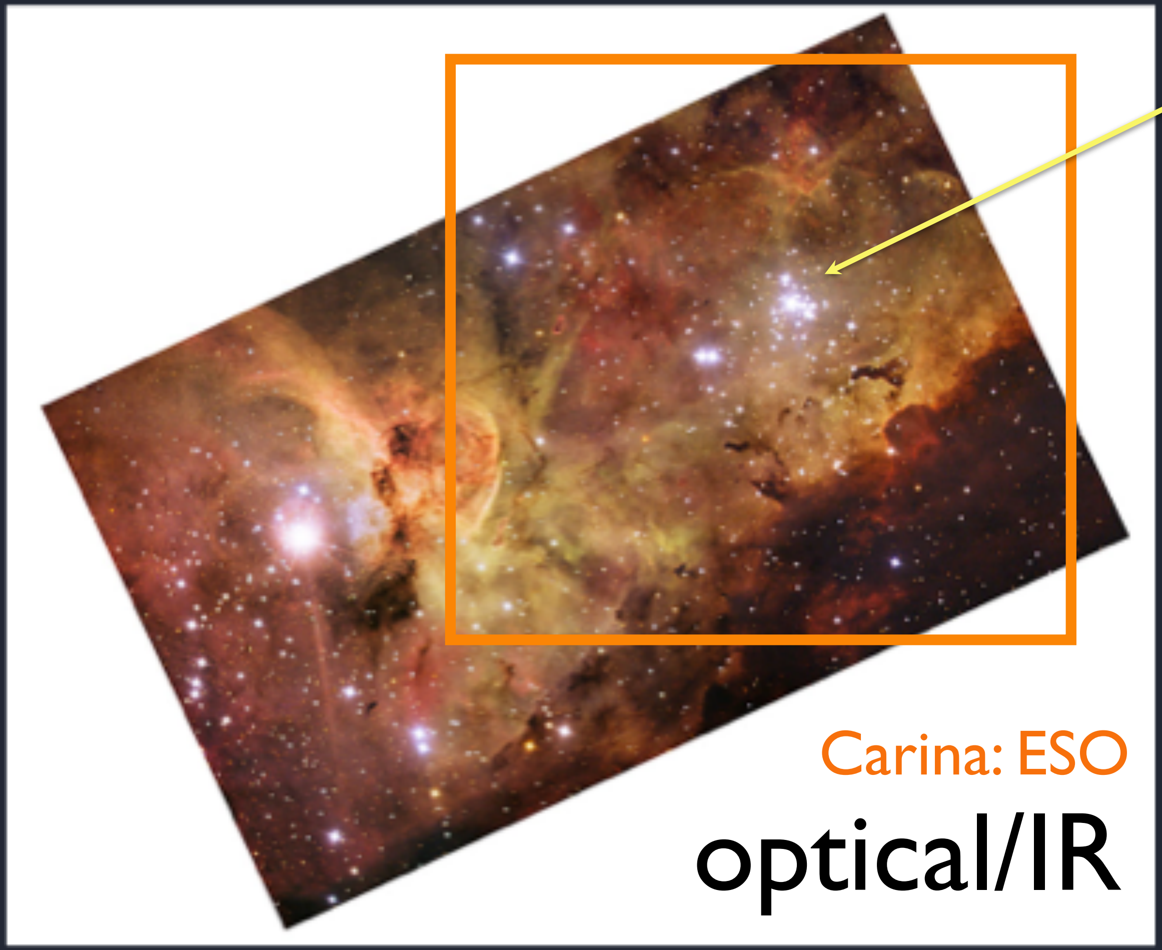

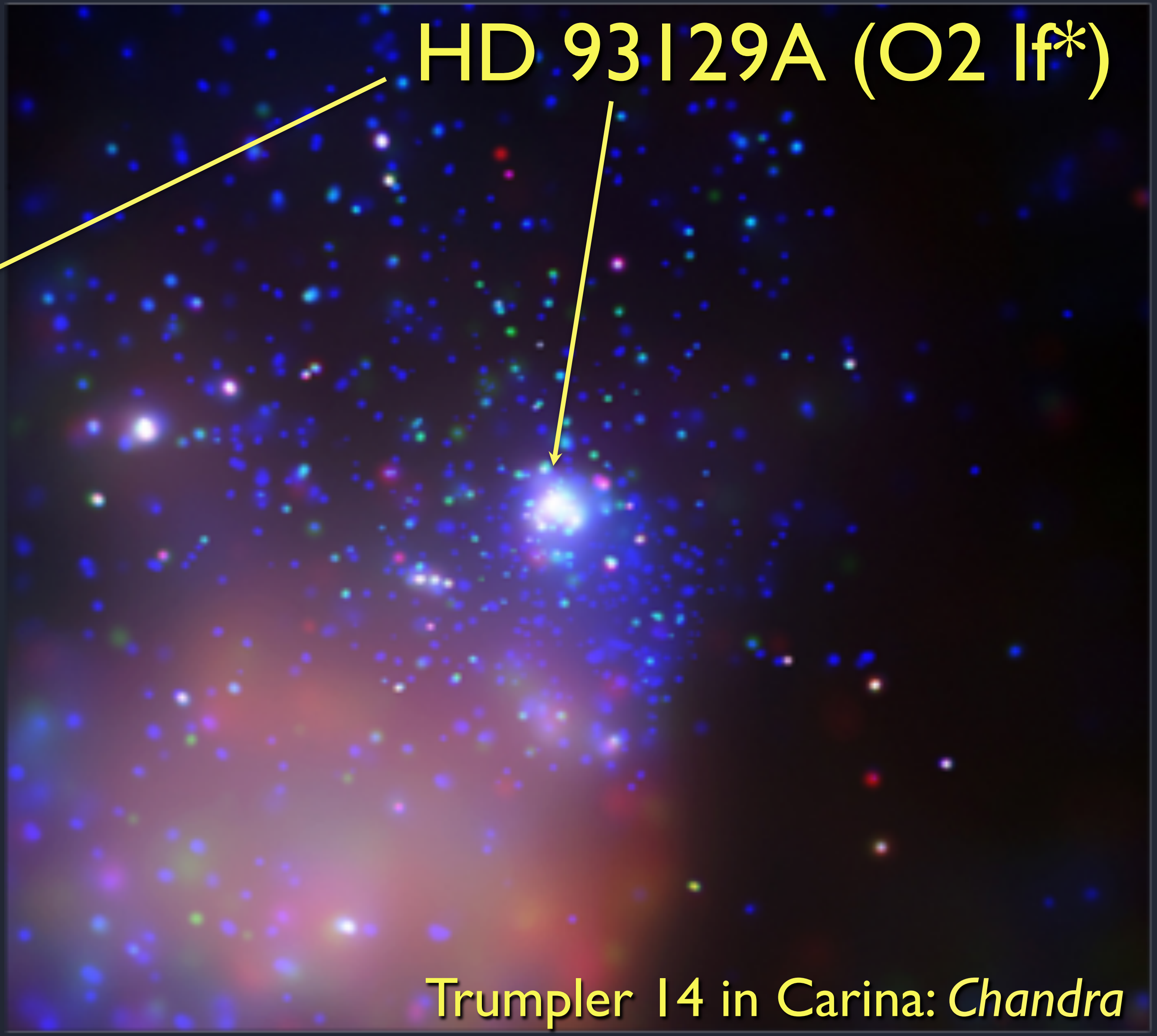

Embedded Wind Shock (EWS) paradigm

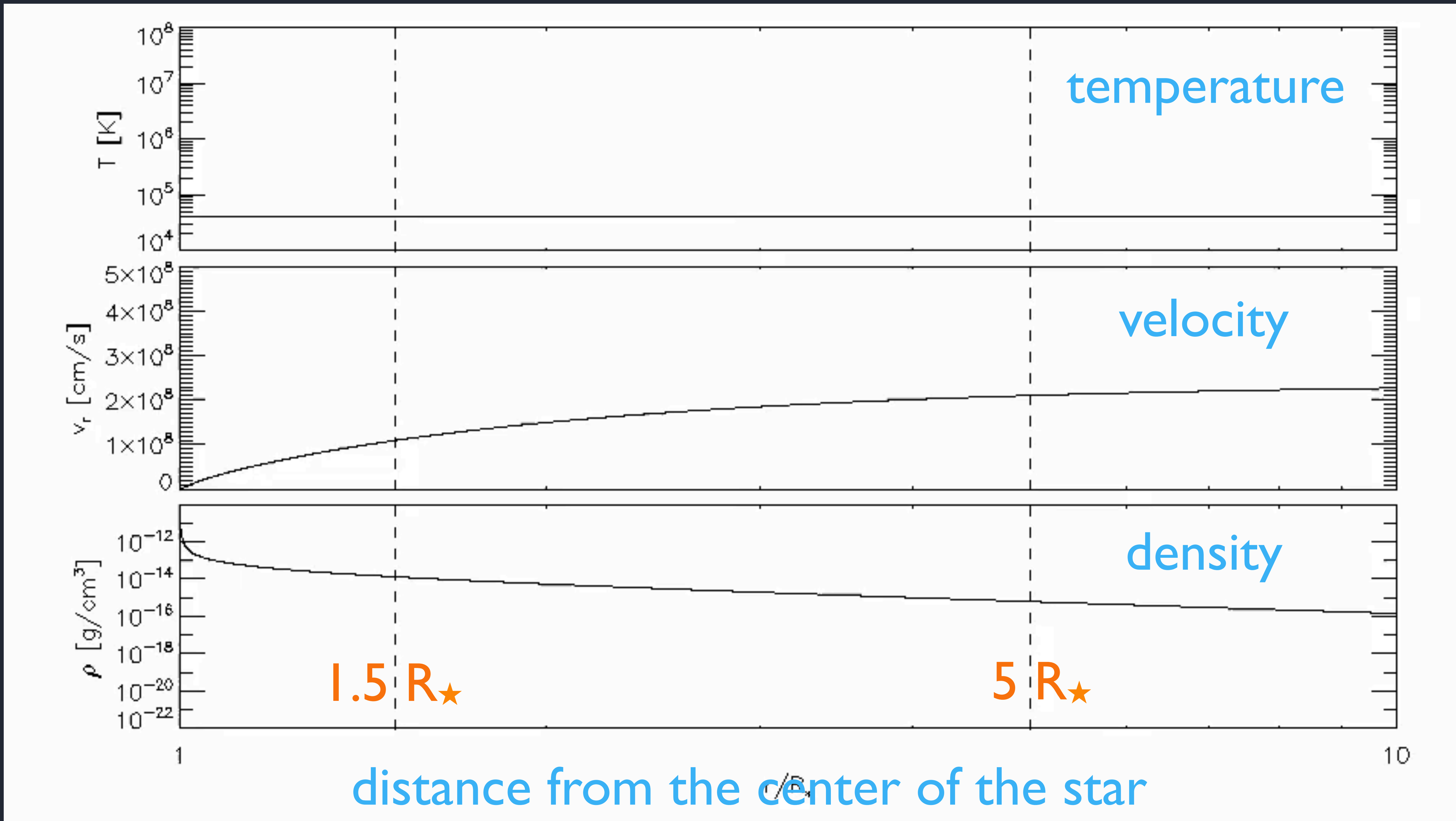

Radiation-hydrodynamics simulations (with J. Sundqvist, S. Owocki, Z. Li)

Animaged gif of simulation available at:
astro.swarthmore.edu/~cohen/presentations/movies/ifrc3_abbott0.65_xkovbc350._xmbko1.e-2_epsabs-1.e-20.gif

Line-Deshadowing Instability (LDI)

LDI (Milne 1926) is intrinsic to any radiation-driven outflow in which the momentum transfer is mediated by spectral lines

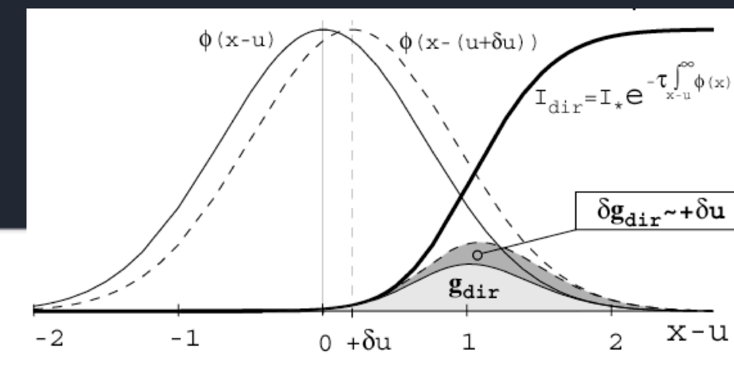

rapidly accelerating material is out of the Doppler shadow of the material behind it

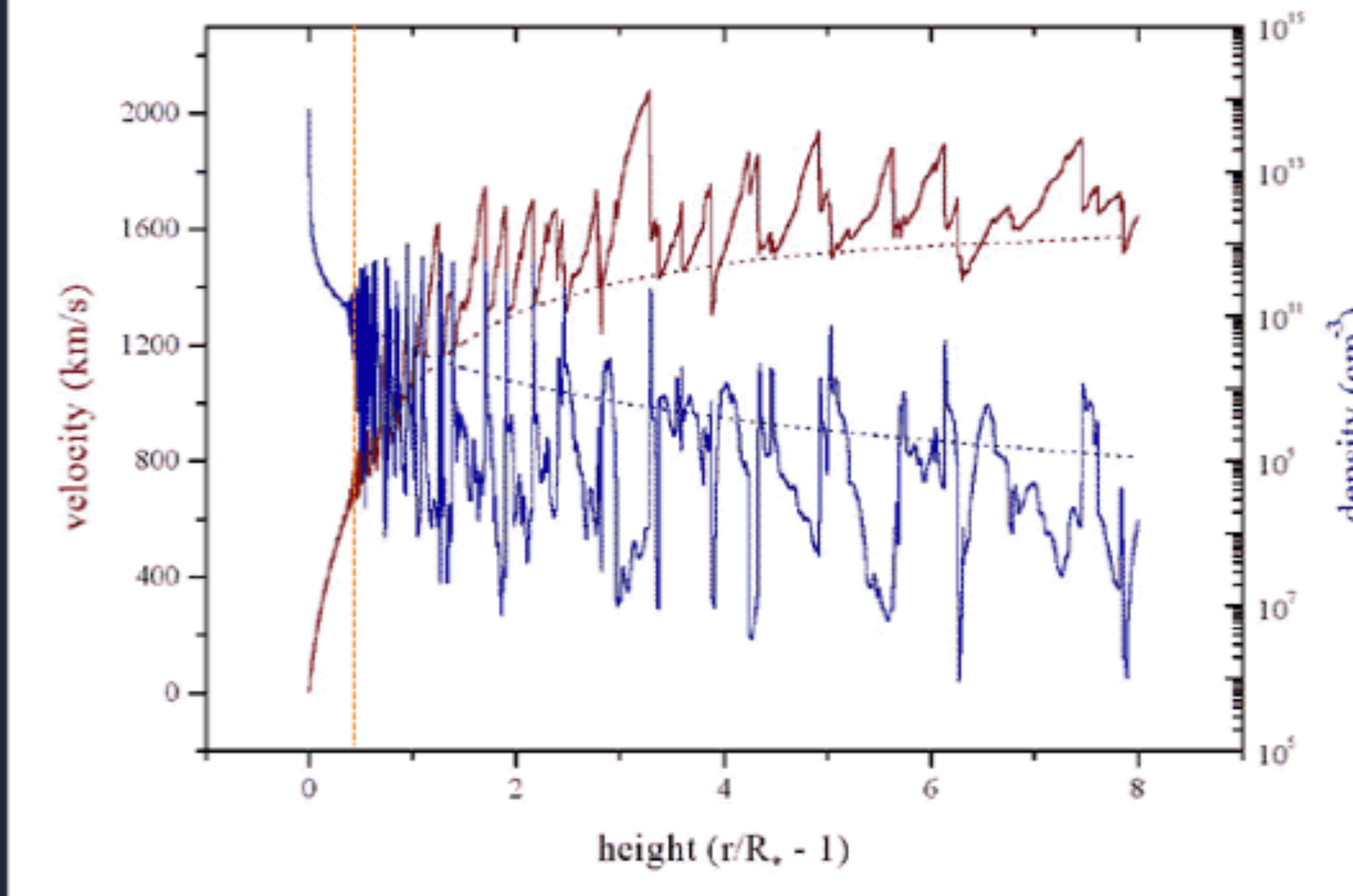

Less than 1% of the mass of the wind is emitting X-rays

>99% of the wind is cold and X-ray *absorbing*

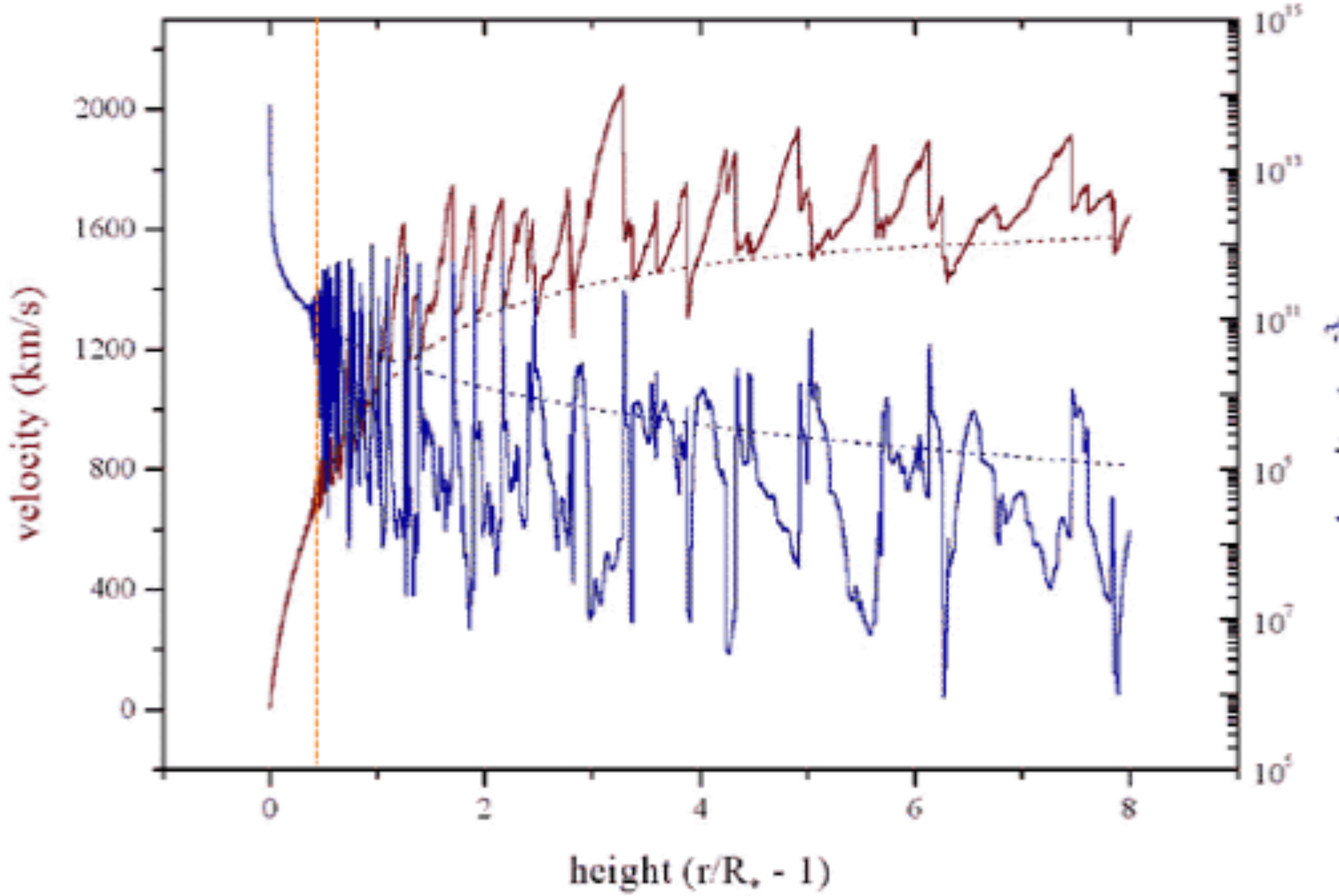

Chandra grating spectra confirmed the EWS scenario

$V_{Doppler} \sim V_{wind}$

zeta Pup (O4 If): 63 ks *Chandra* MEG

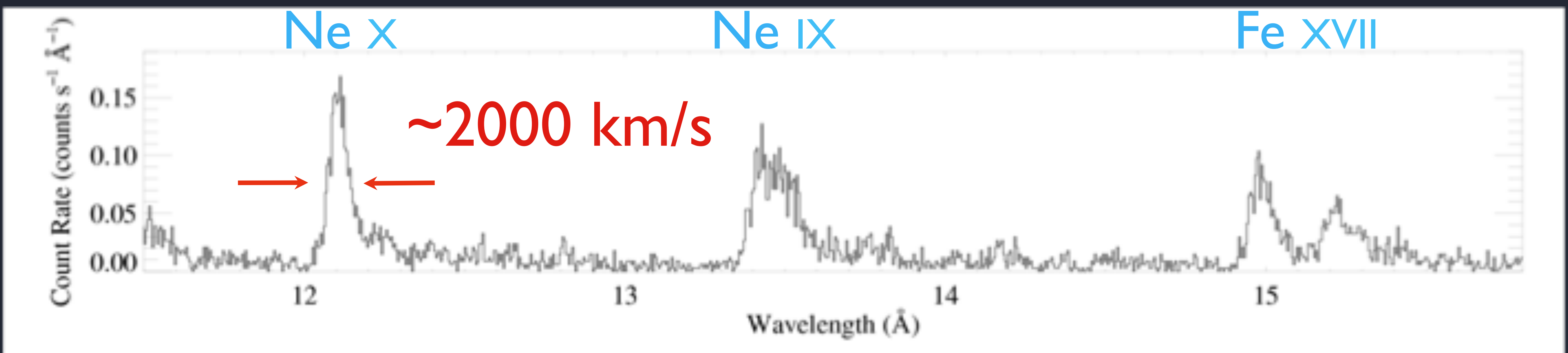

Chandra easily resolves the wind-broadened X-ray emission lines

Chandra Medium Energy Grating (MEG)

ζ Pup (O4 If)

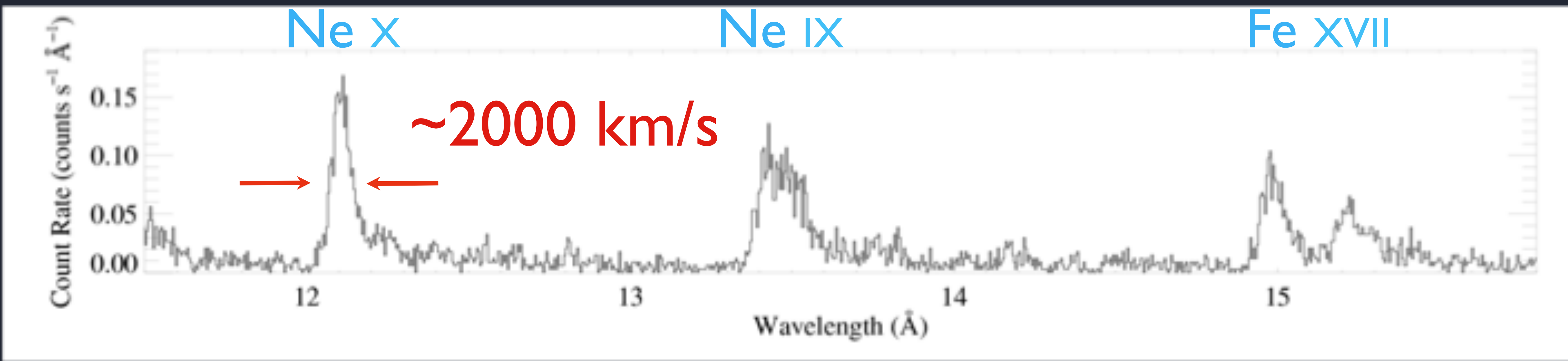

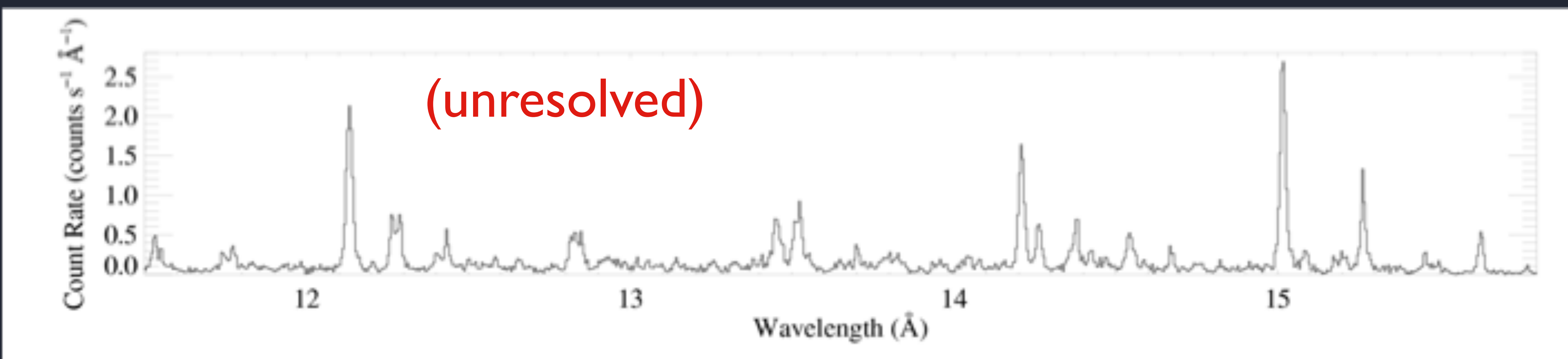

Capella (G5 III)

lines are *asymmetric:*

this is a signature of wind absorption, and enables us to *measure the wind mass-loss rate*

ζ Pup (O4If)

Capella (G5 III)

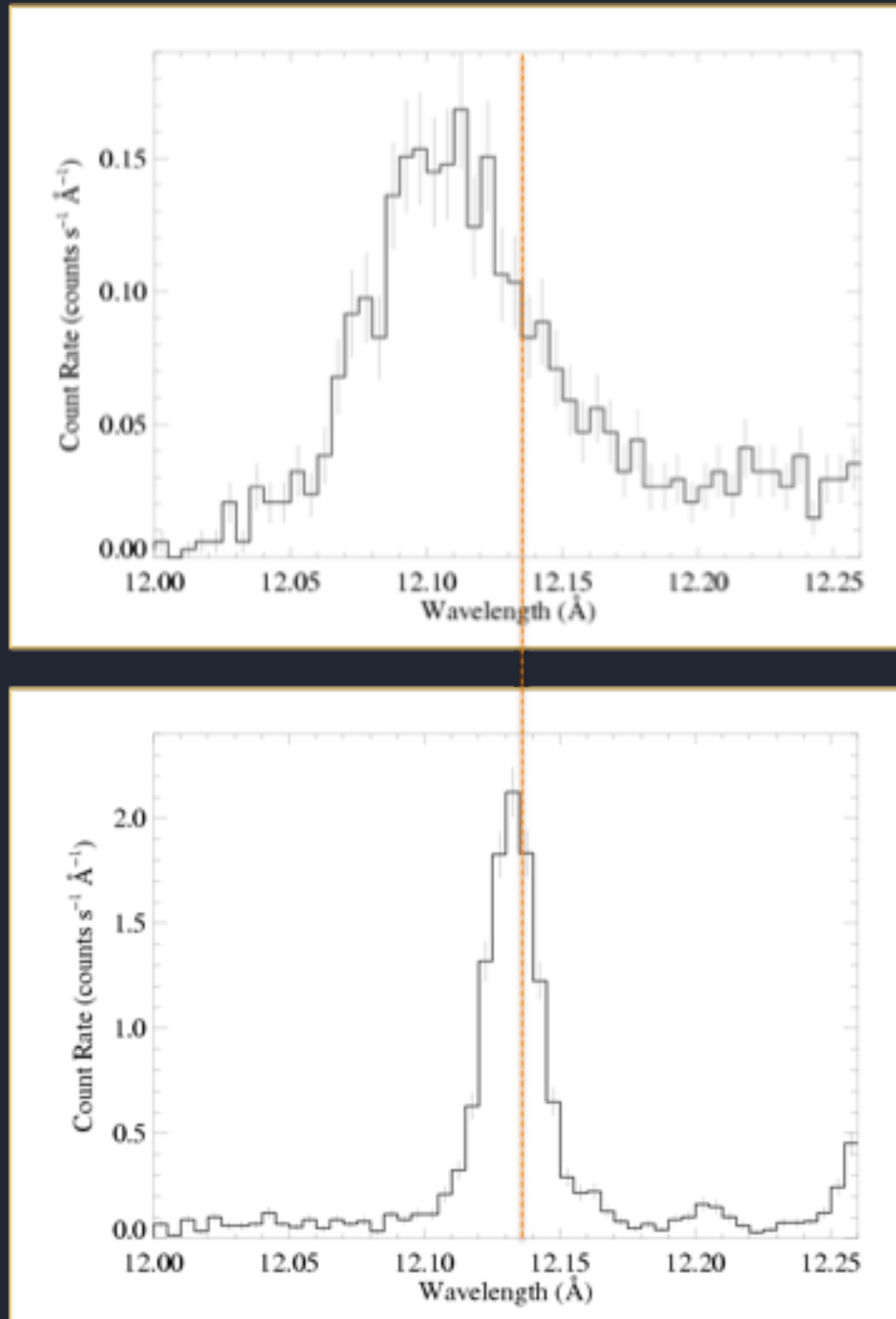

$v = v_\infty(1 - r/R_\star)^\beta$

beta velocity law assumed

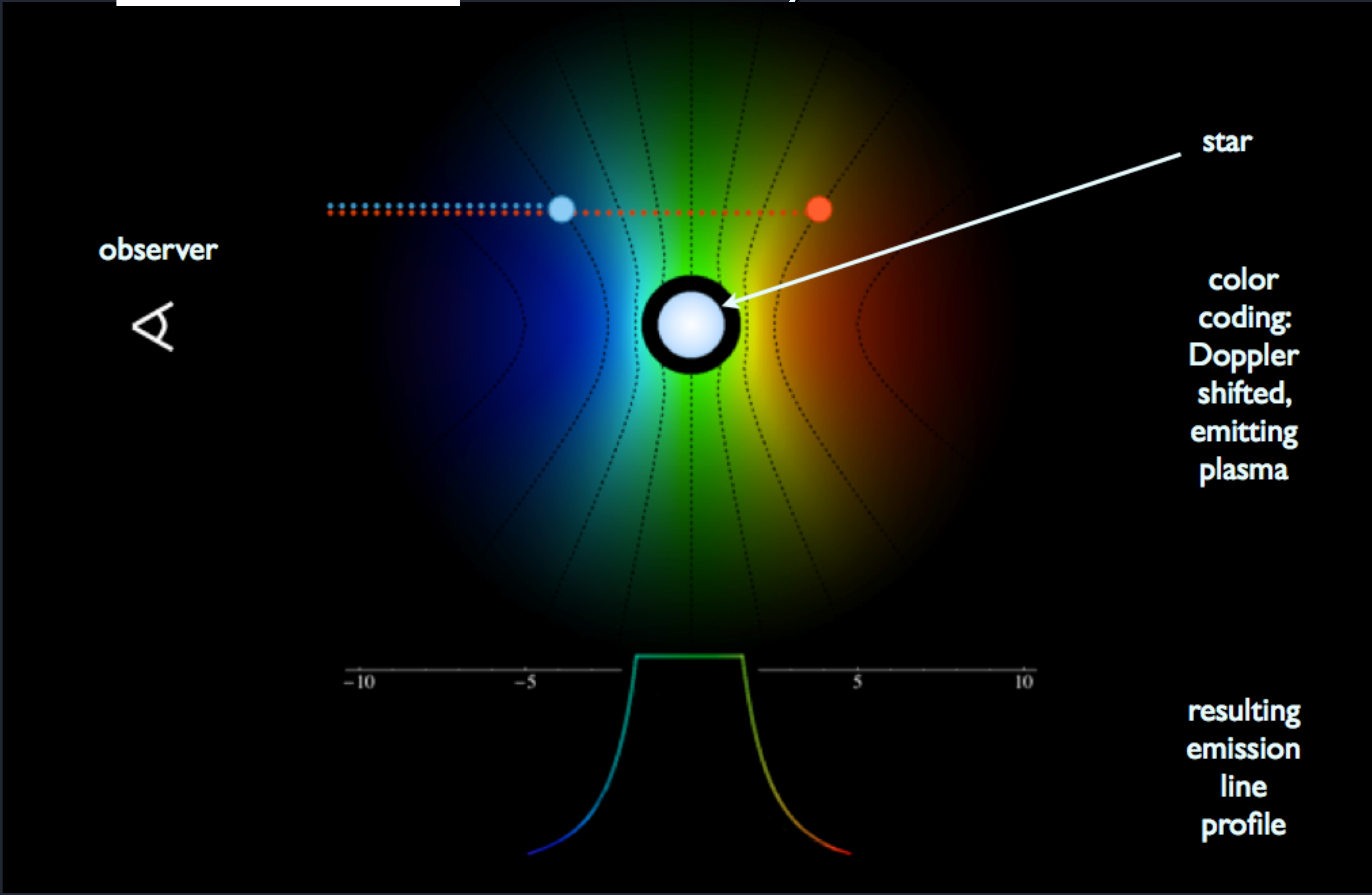

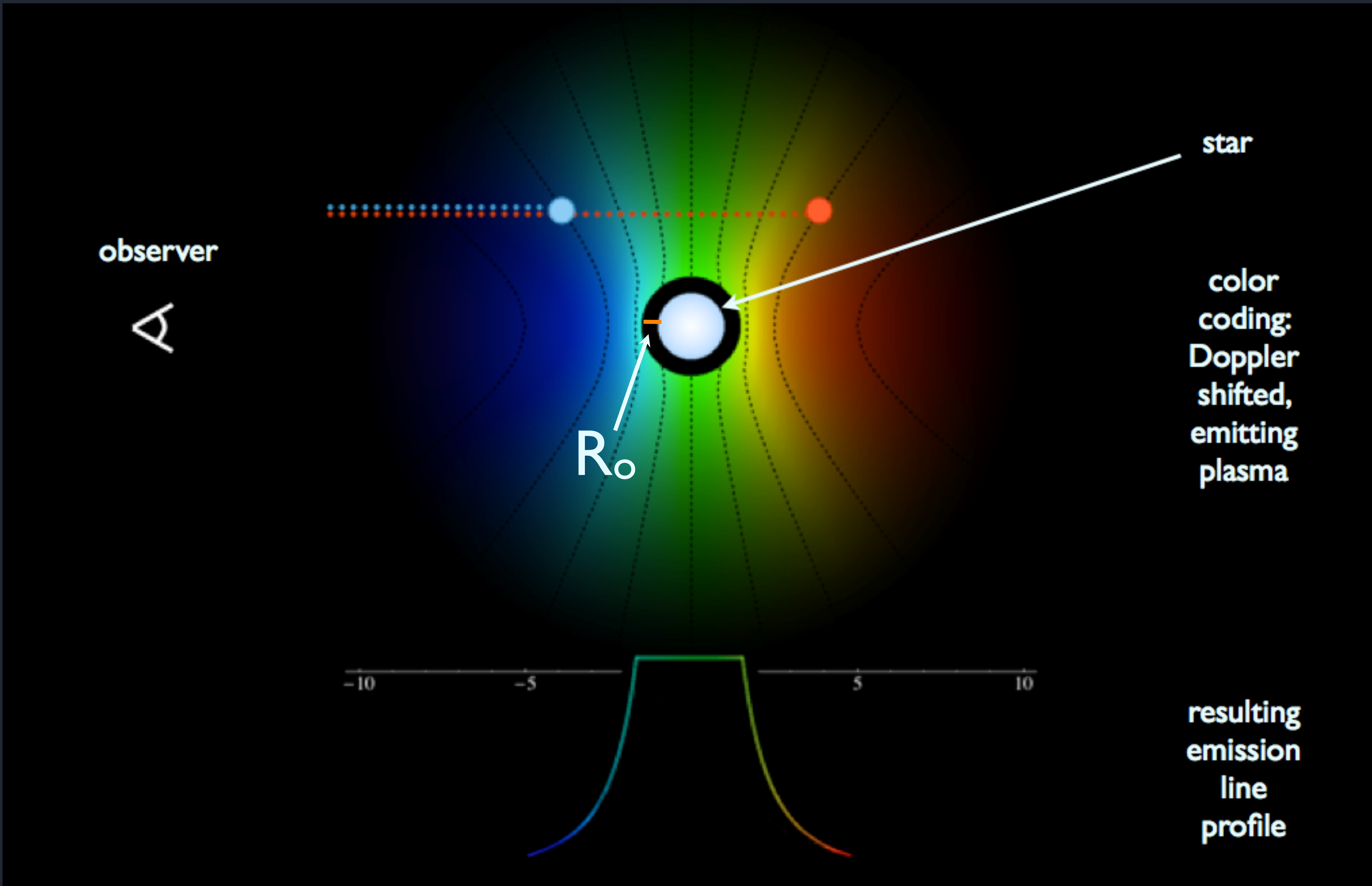
observer
star
R_o
color coding: Doppler shifted, emitting plasma
−10
−5
5
10
resulting emission line profile

Line Asymmetry

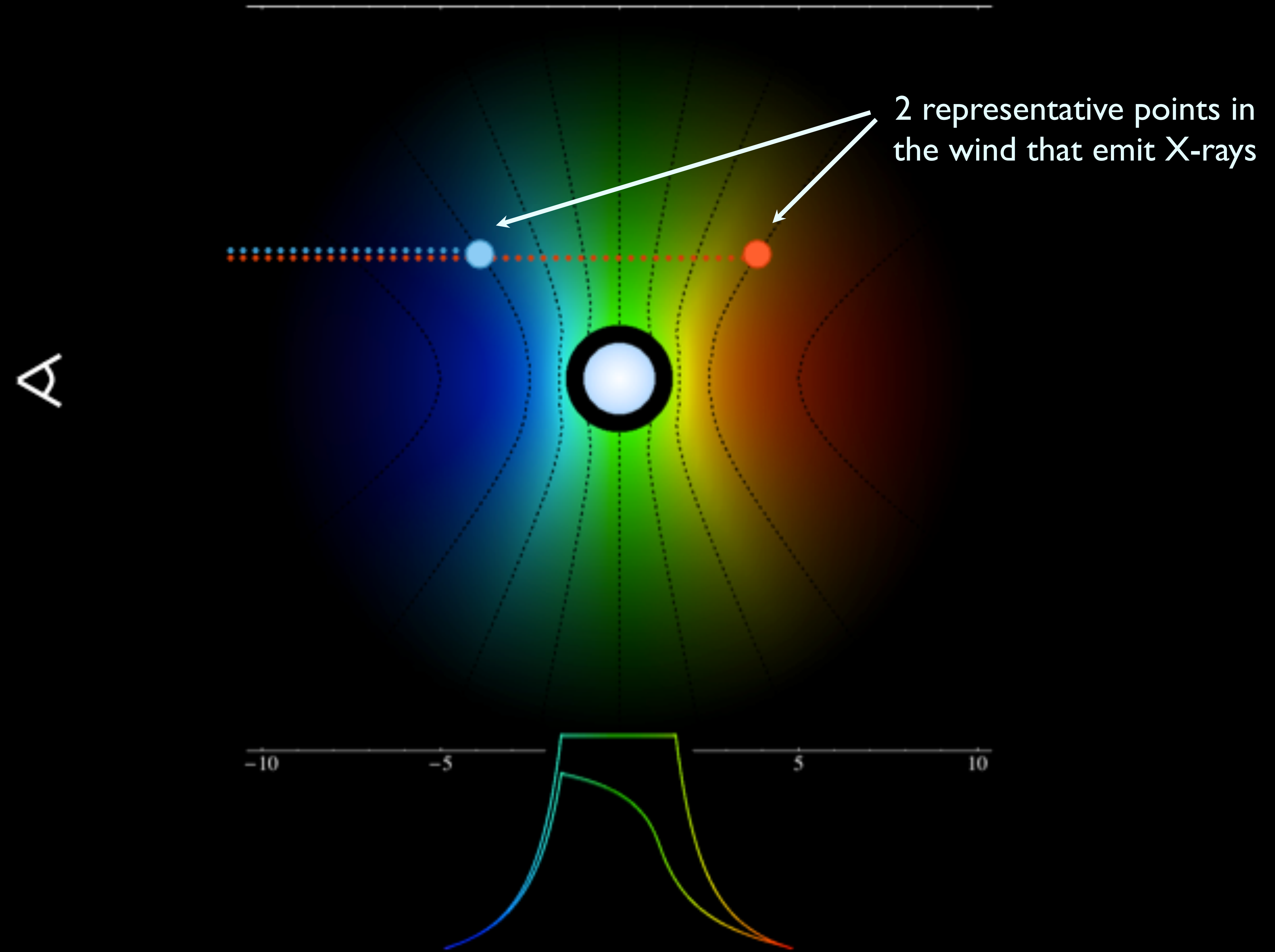

Line Asymmetry

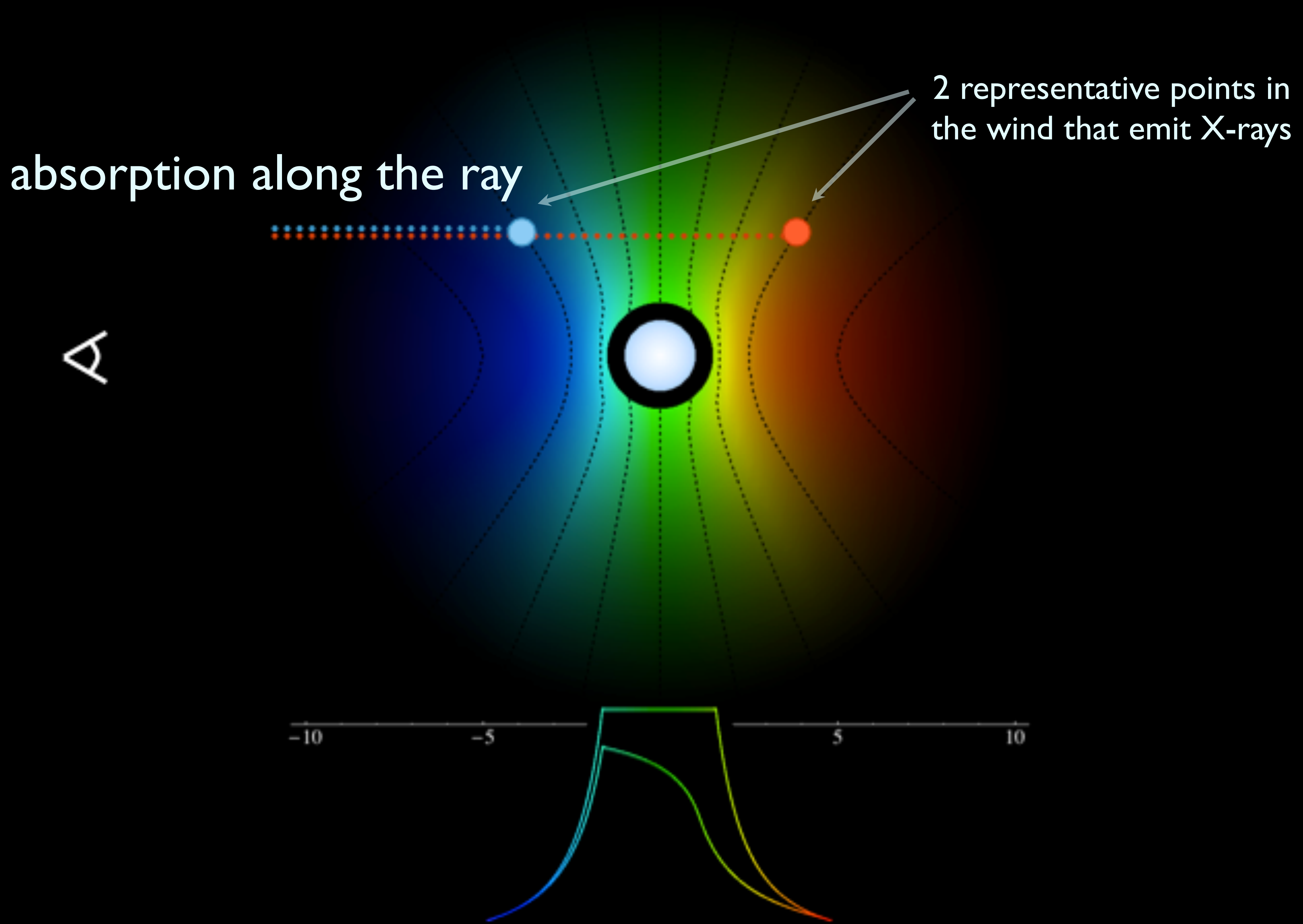

Line Asymmetry

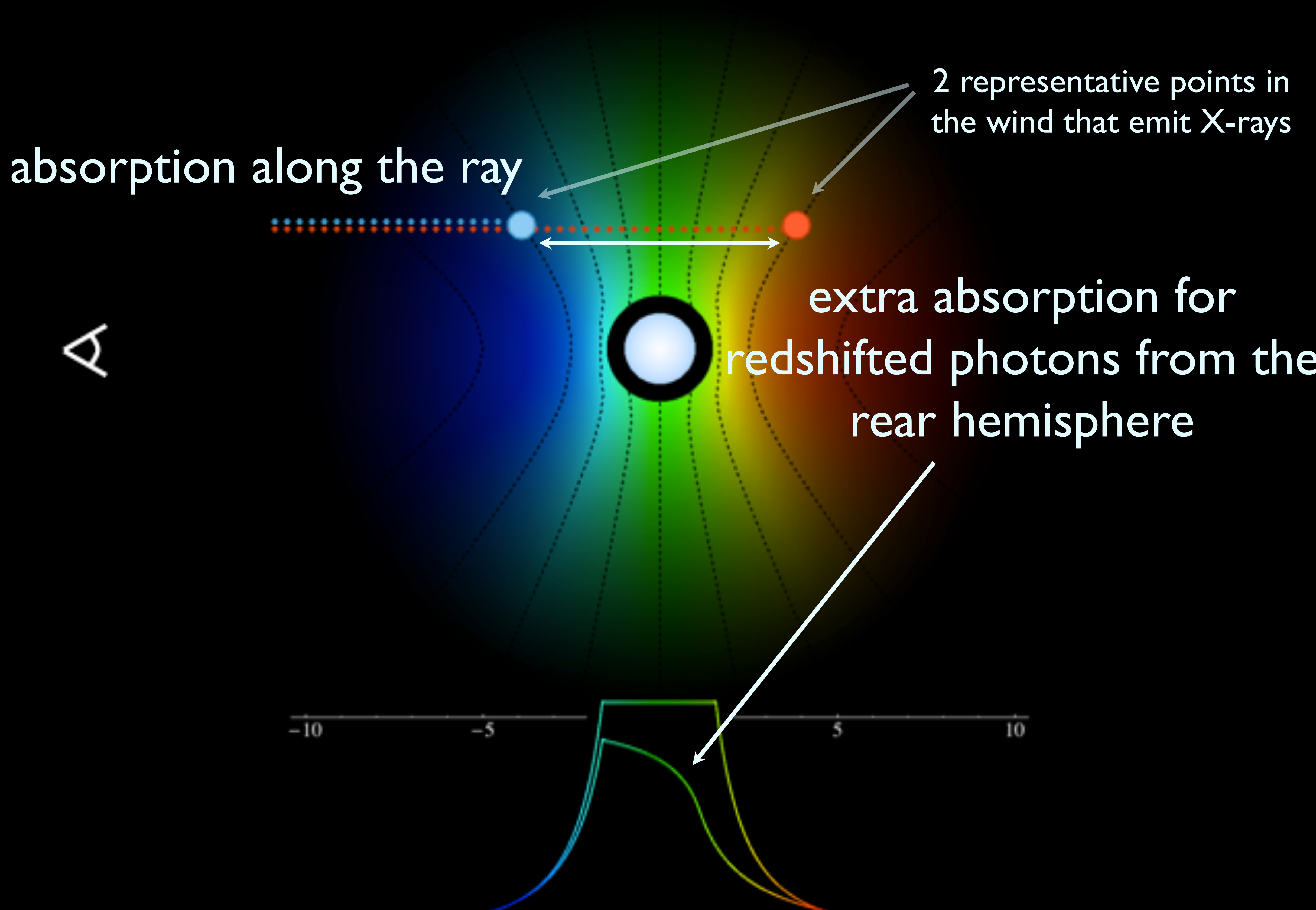

Wind Profile Model

mass-loss rates ~10^{-6}: expect wind to be modestly optically thick

$$\tau_* = \frac{\kappa \dot{M}}{4\pi R_* v_\infty}$$

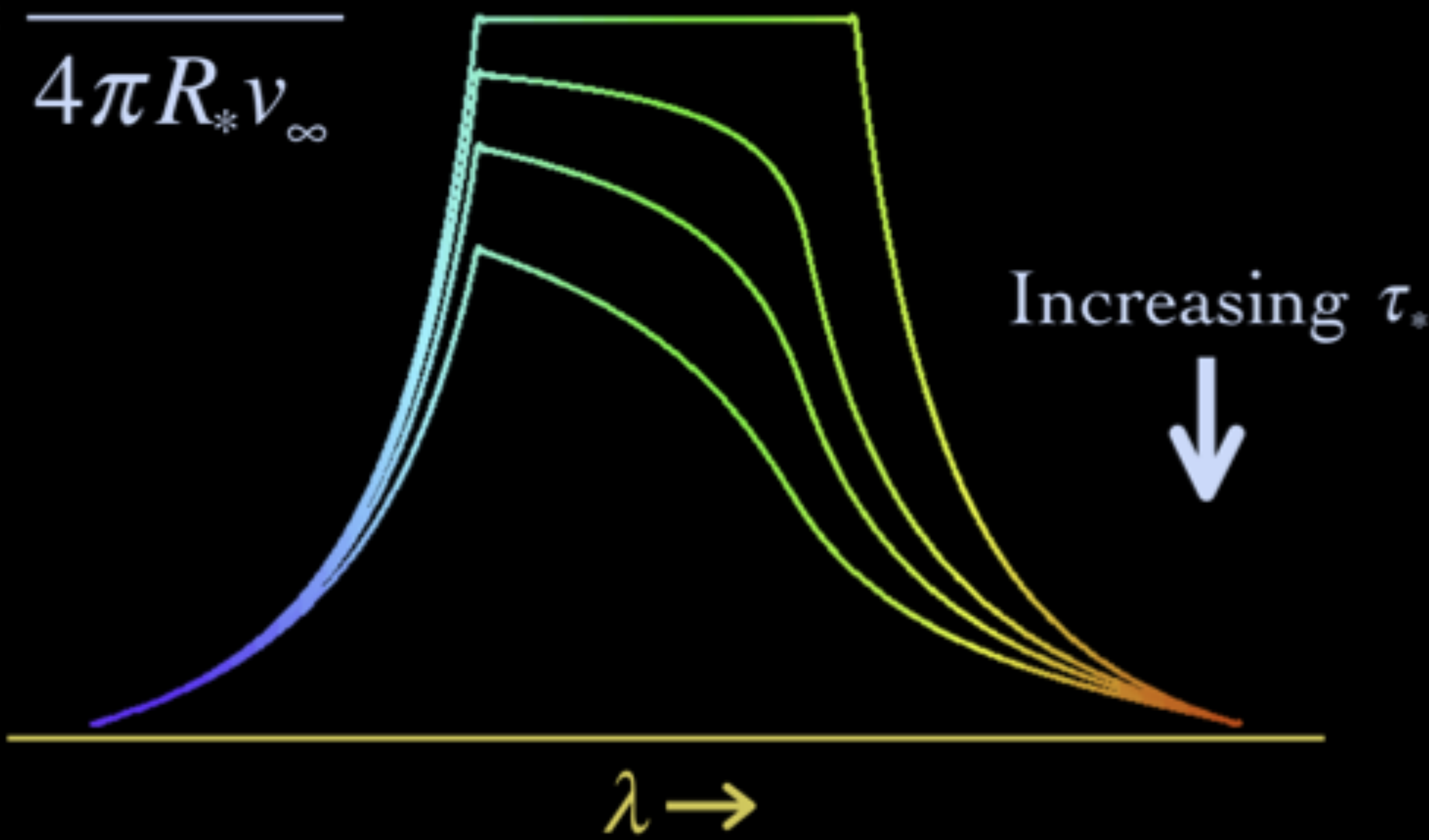

Line profile shapes

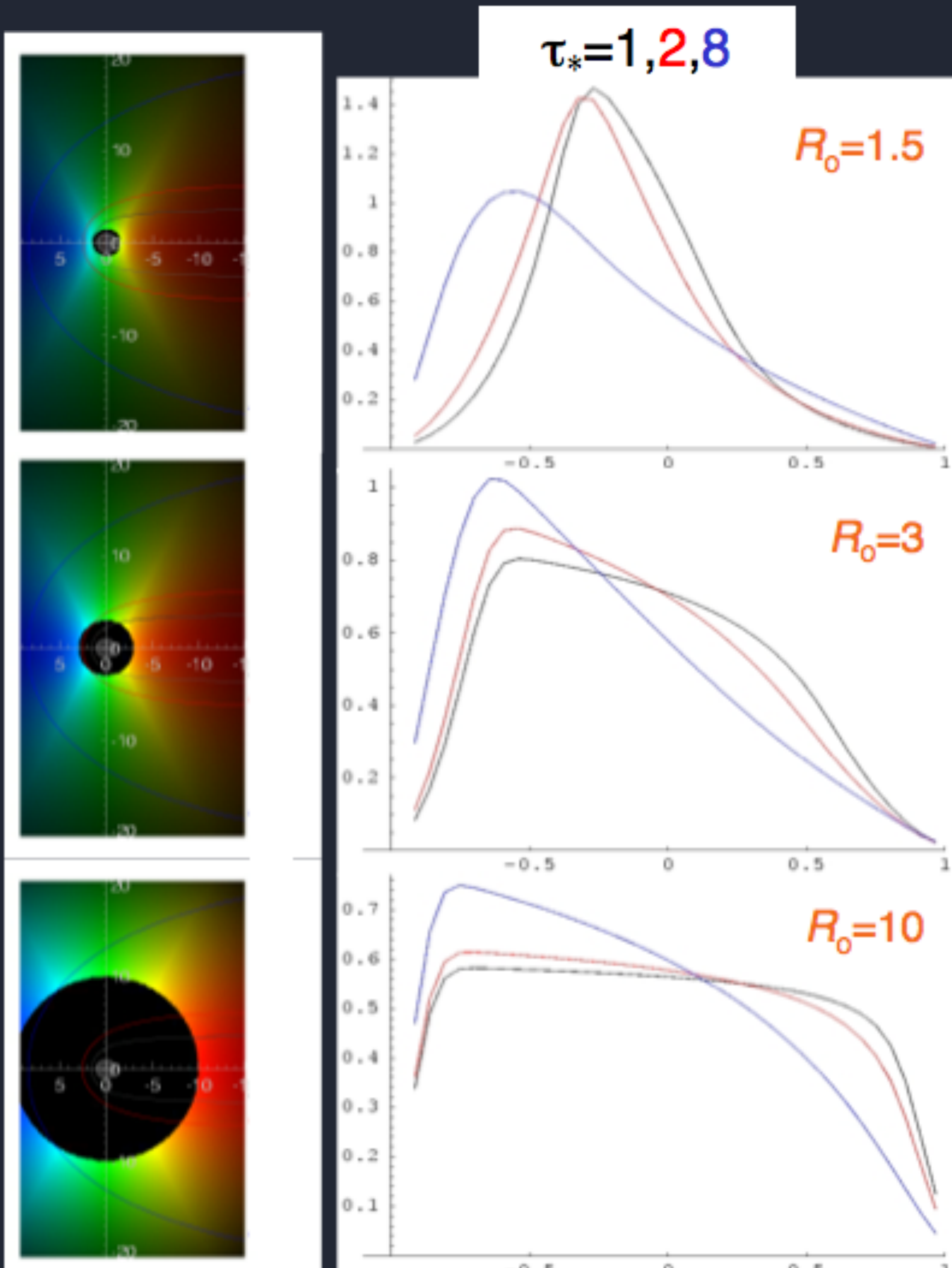

key parameters: R_o & $\tau_\star$

$$v = v_\infty(1-r/R_\star)^\beta$$

$j \sim \rho^2$ for $r/R_\star > R_o$,

$= 0$ otherwise

$$\tau = \tau_* \int_z^\infty \frac{R_* dz'}{r'^2 (1-\frac{R_*}{r'})^\beta}$$

$$\tau_* \equiv \frac{\kappa \dot{M}}{4\pi R_* v_\infty}$$

Owocki & Cohen 2001

Fit the model to data

ζ Pup: *Chandra*

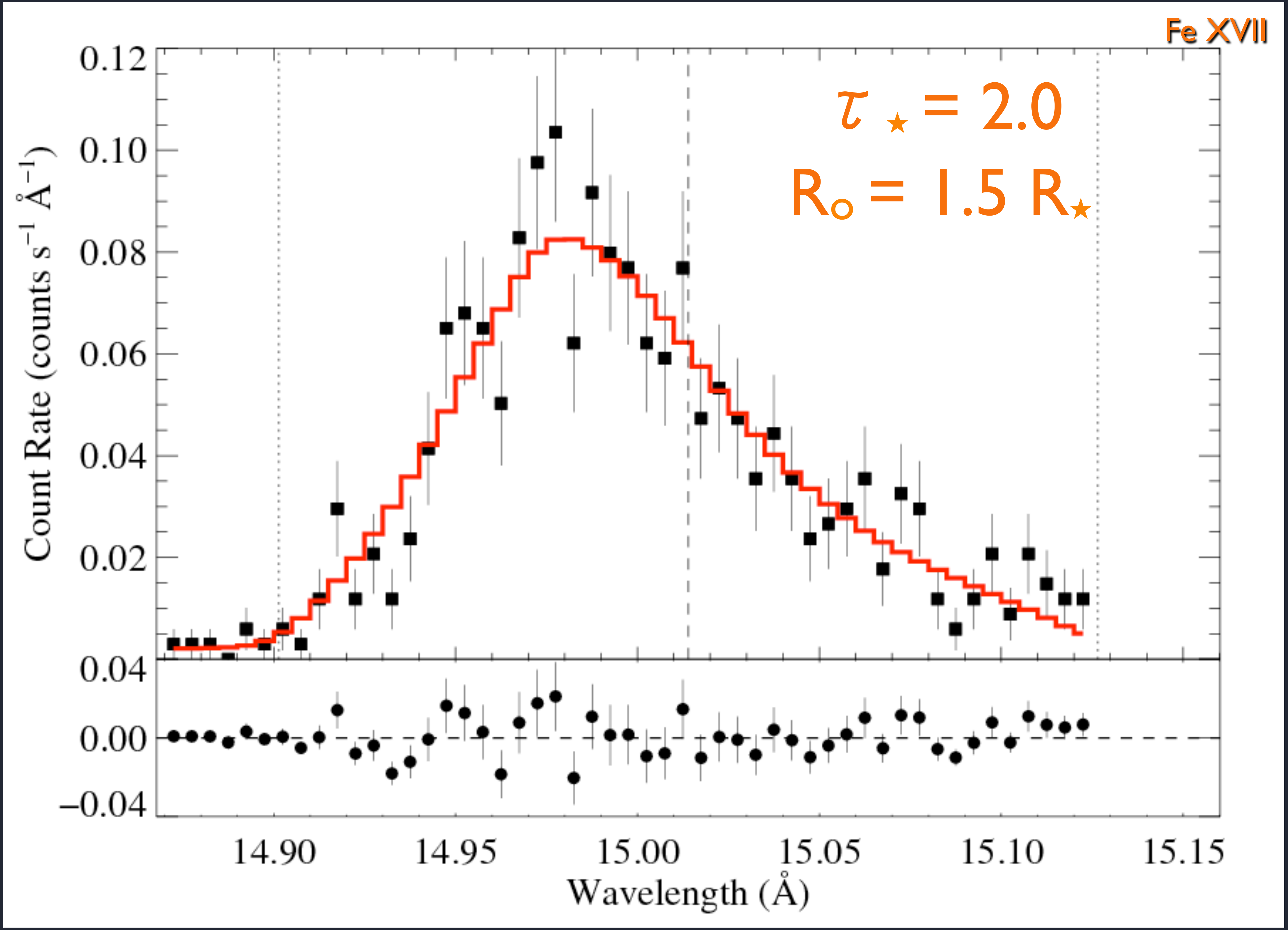

Distribution of R_o values for ζ Pup

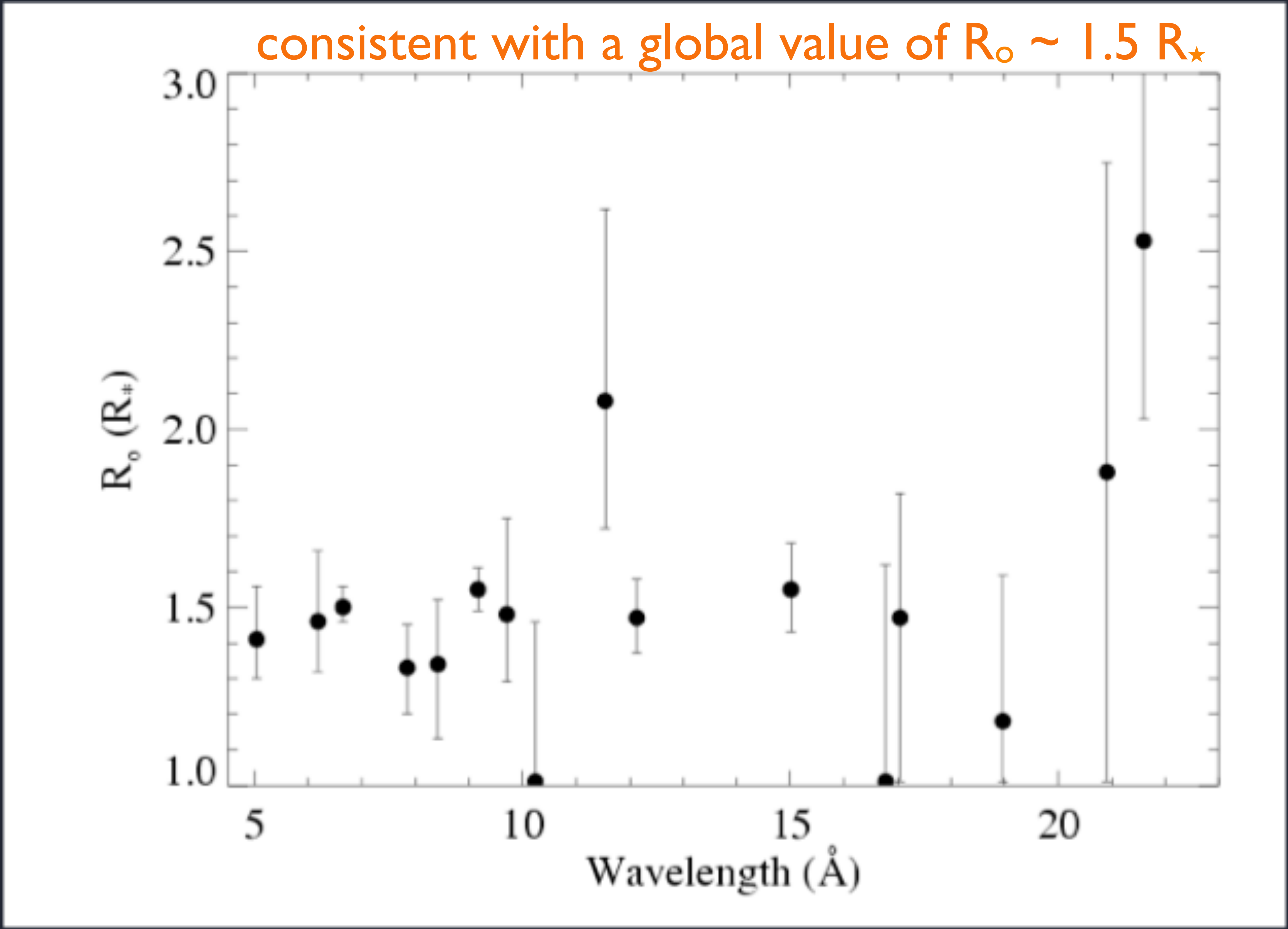

Fit the model to data

ζ Pup: *Chandra*

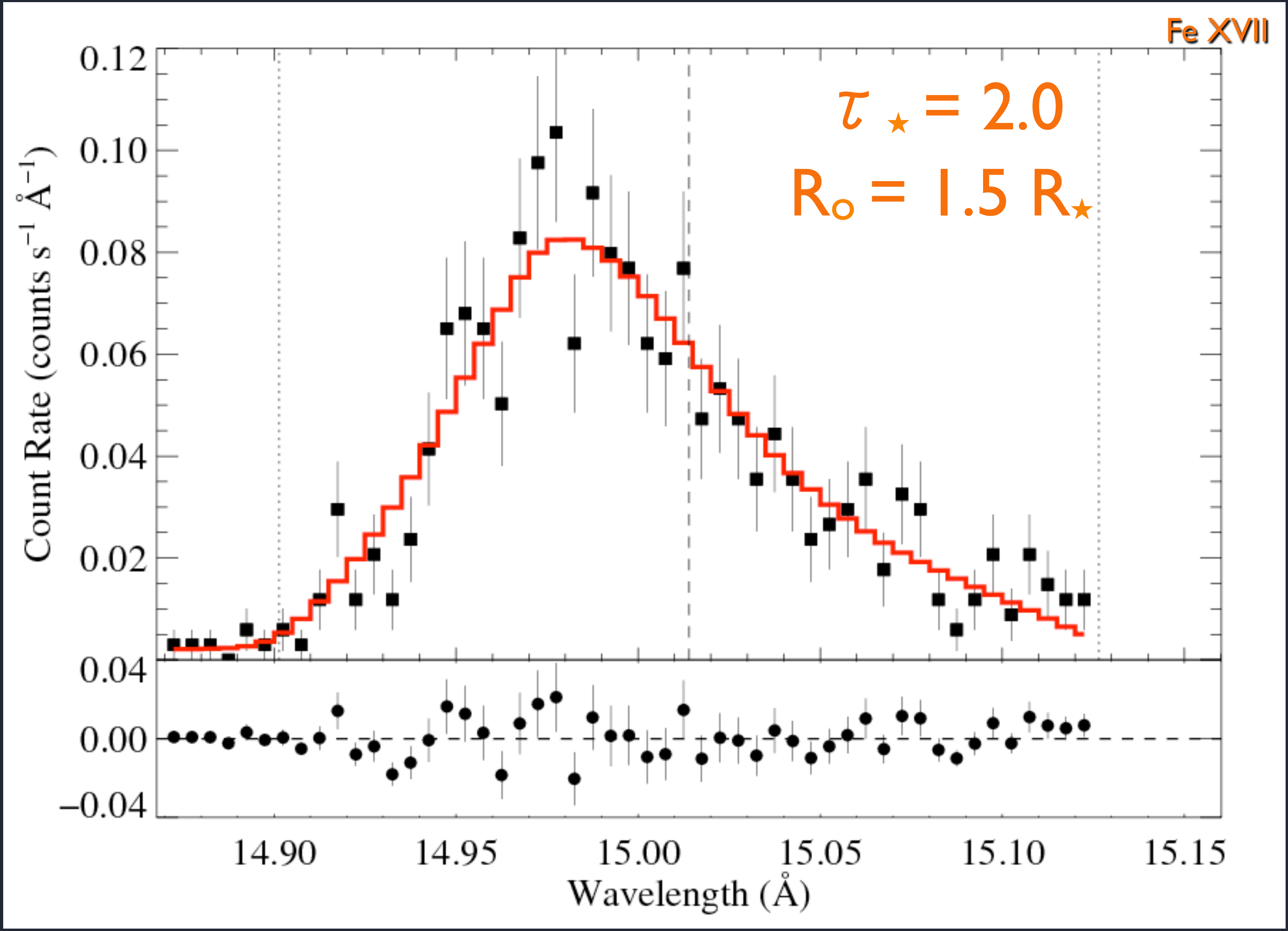

Quantifying the wind optical depth

opacity of the cold wind component (due to photoionization of C, N, O, Ne, Fe)

wind mass-loss rate

$$\dot{M} = 4\pi r^2 v \rho$$

$$\tau_* \equiv \frac{\kappa \dot{M}}{4\pi R_* v_\infty}$$

stellar radius

wind terminal velocity

soft X-ray wind opacity

note: absorption arises in the dominant, cool wind component

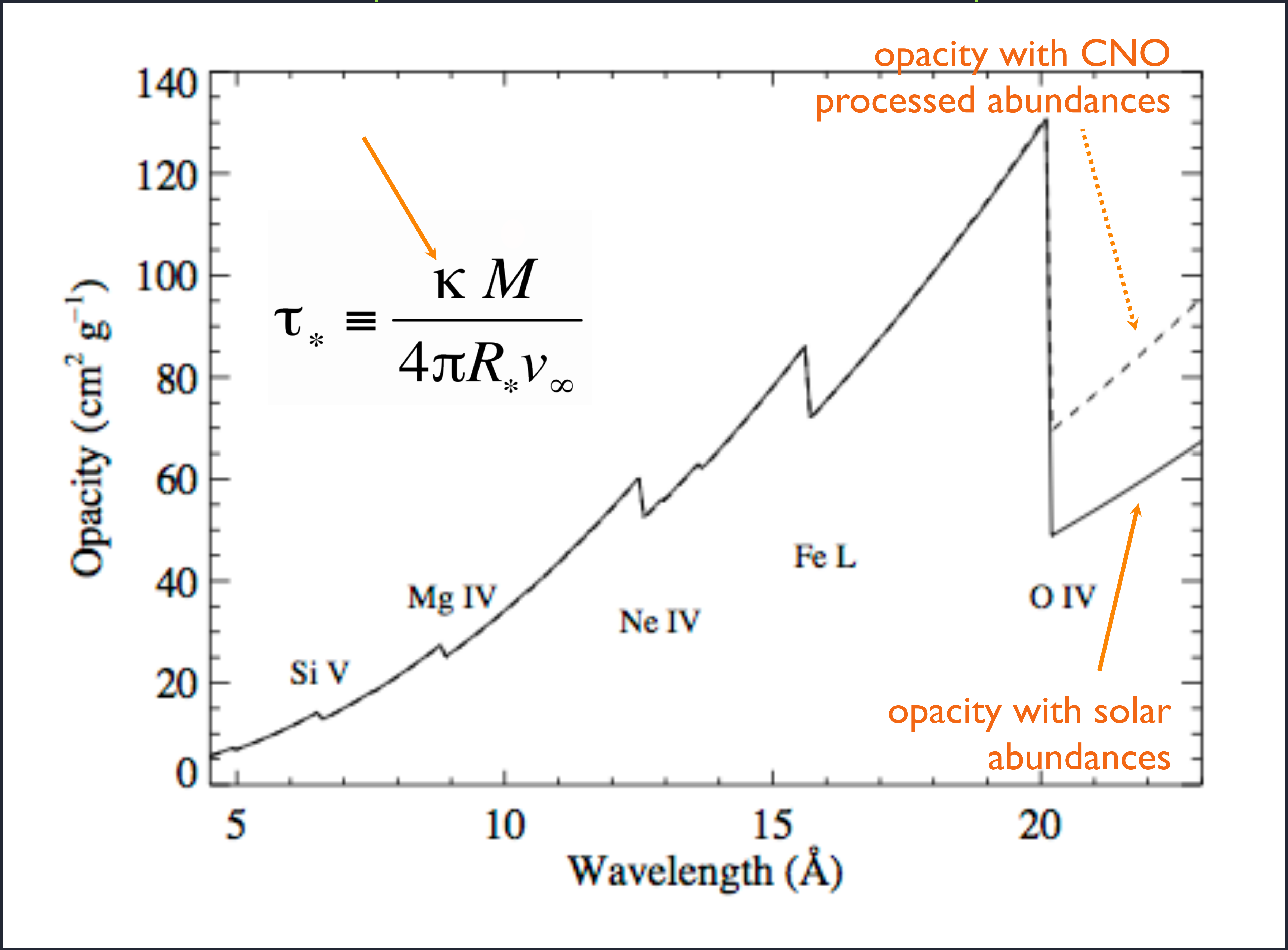

ζ Pup *Chandra*: three emission lines

Mg Ly α : 8.42 Å   Ne Ly α : 12.13 Å   O Ly α : 18.97 Å

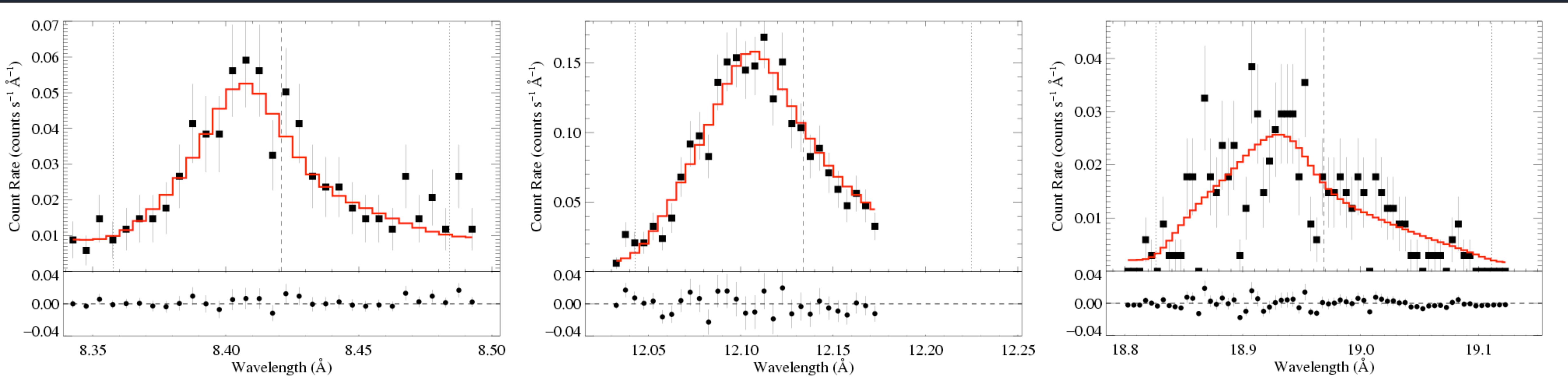

$\tau_* \sim 1$ $\tau_* \sim 2$ $\tau_* \sim 3$

Recall:

$$\tau_* \equiv \frac{\kappa \dot{M}}{4\pi R_* v_\infty}$$

Results from the 3 line fits shown previously

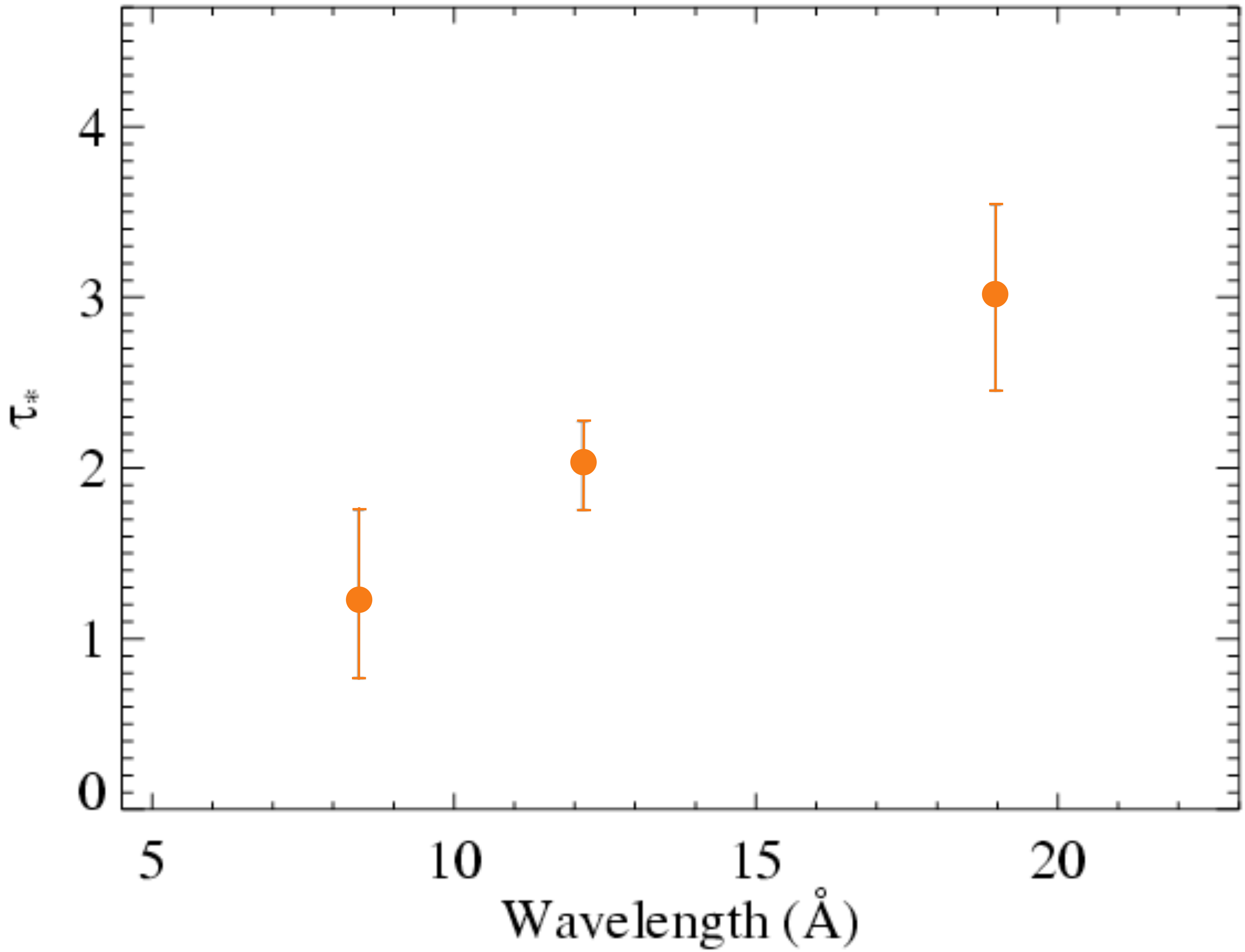

Fits to 16 lines in the *Chandra* spectrum of ζ Pup

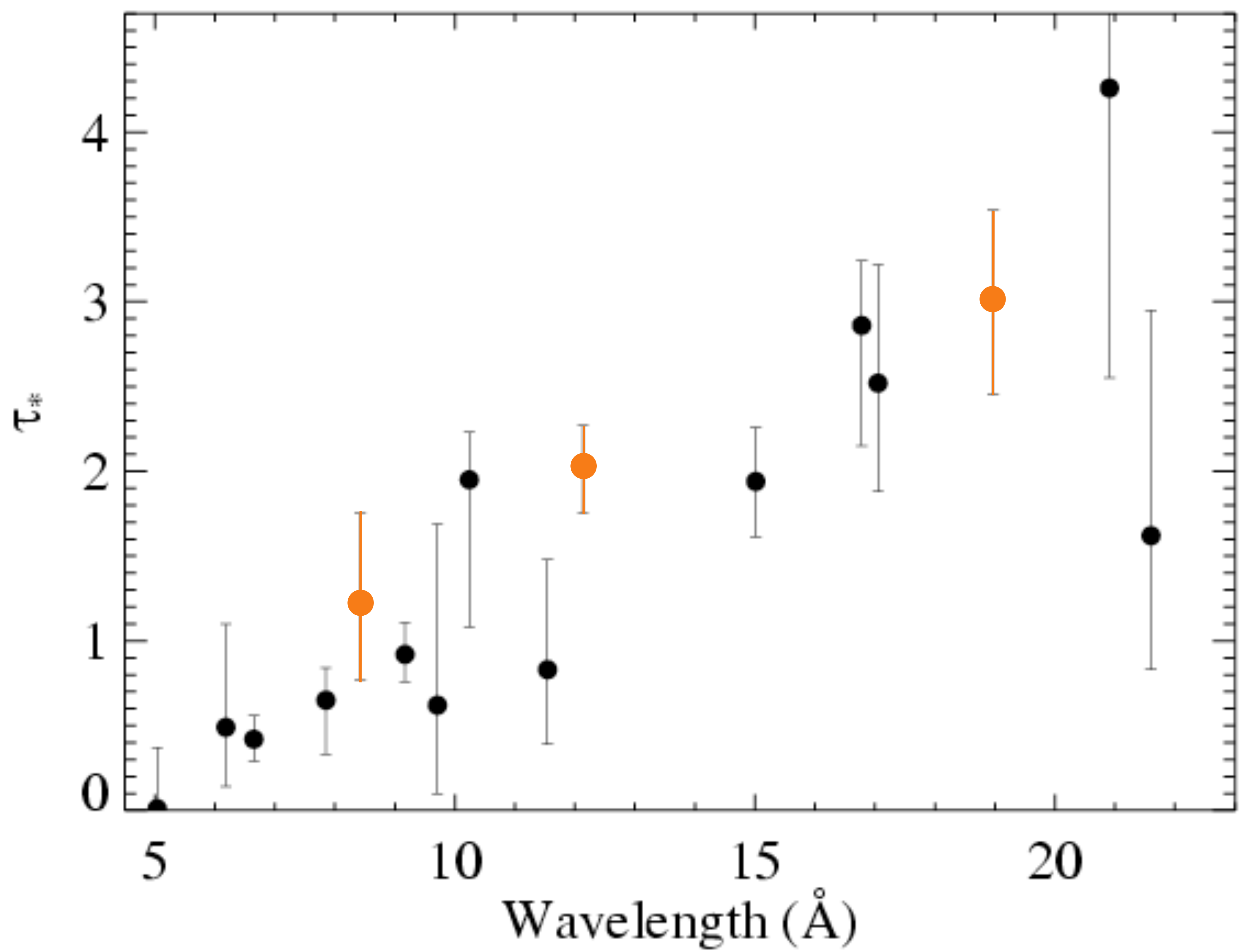

Fits to 16 lines in the *Chandra* spectrum of ζ Pup

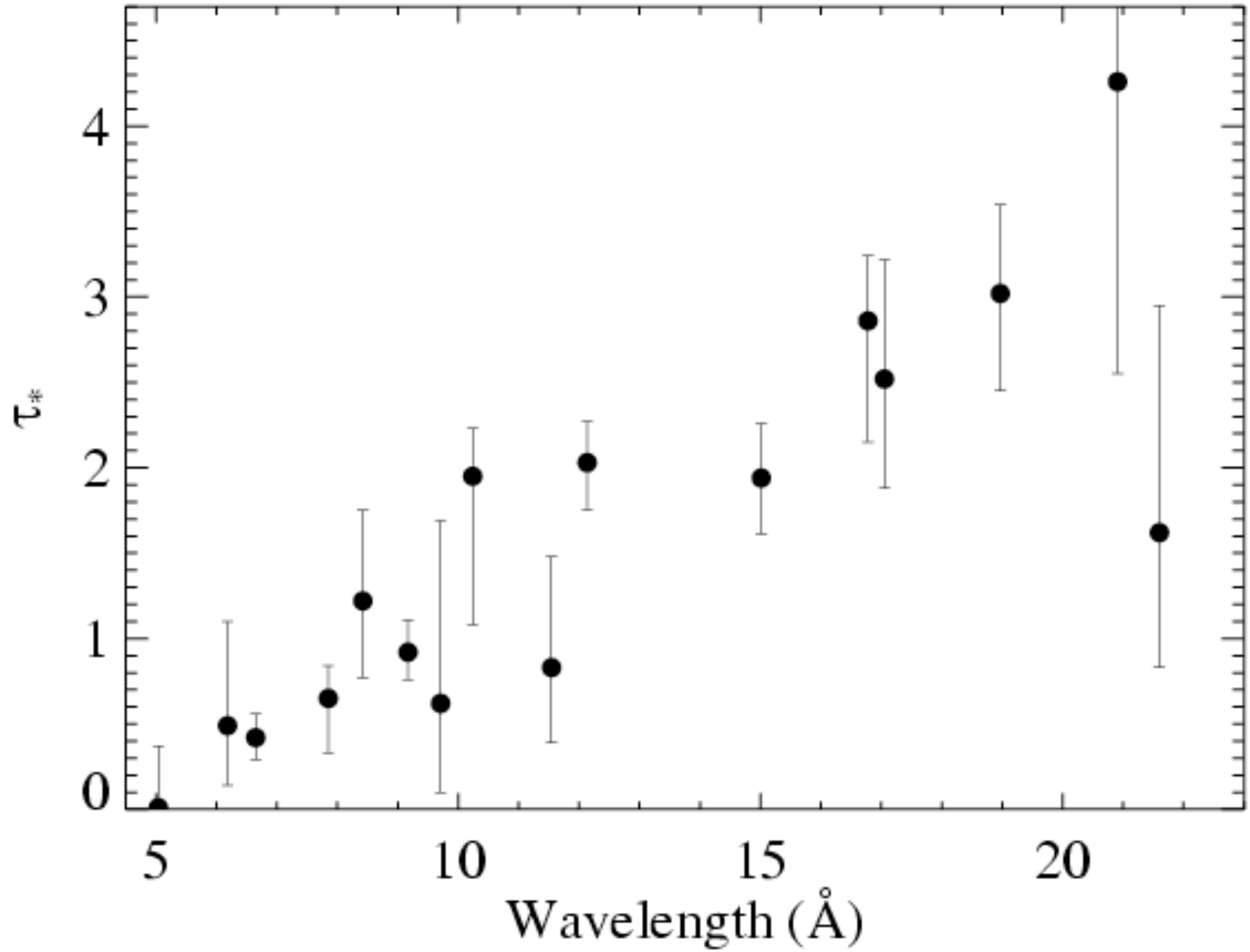

Fits to 16 lines in the *Chandra* spectrum of ζ Pup

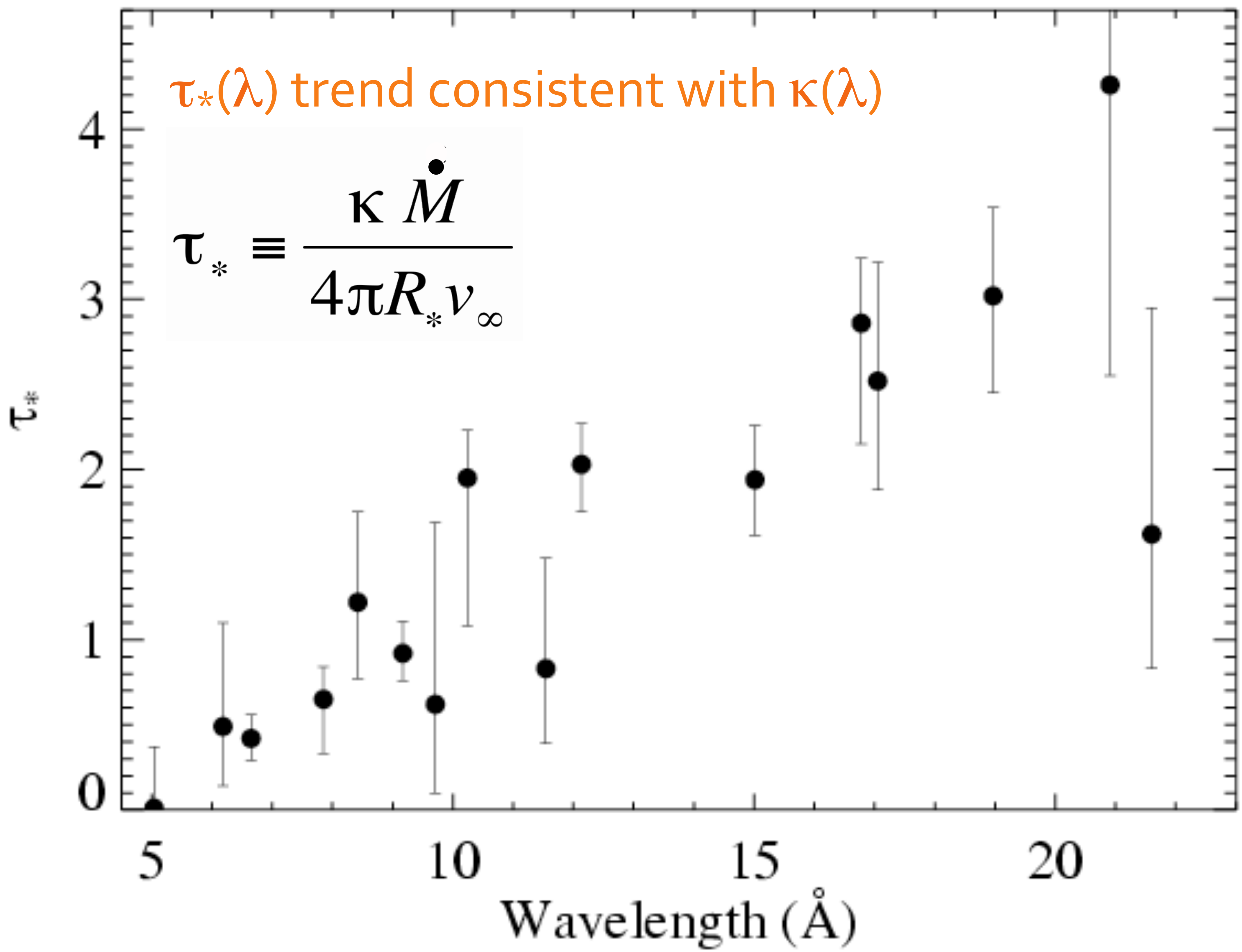

$$\tau_* \equiv \frac{\kappa \dot{M}}{4\pi R_* v_\infty}$$

$\dot{M}$ becomes the free parameter of the **fit** to the $\tau_*(\lambda)$ trend

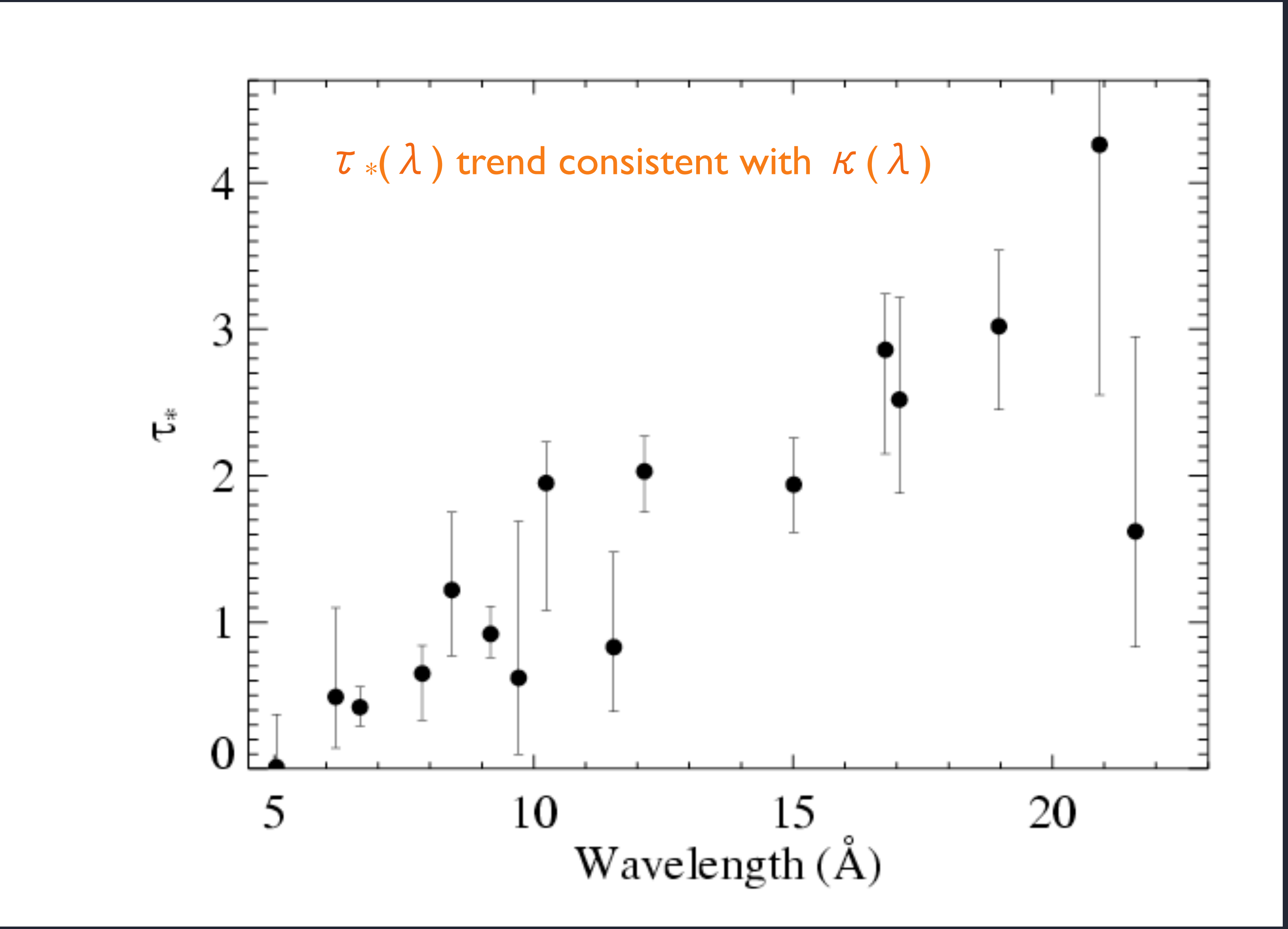

$$\tau_* \equiv \frac{\kappa \dot{M}}{4\pi R_* v_\infty}$$

$\dot{M}$ becomes the free parameter of the **fit** to the $\tau_*(\lambda)$ trend

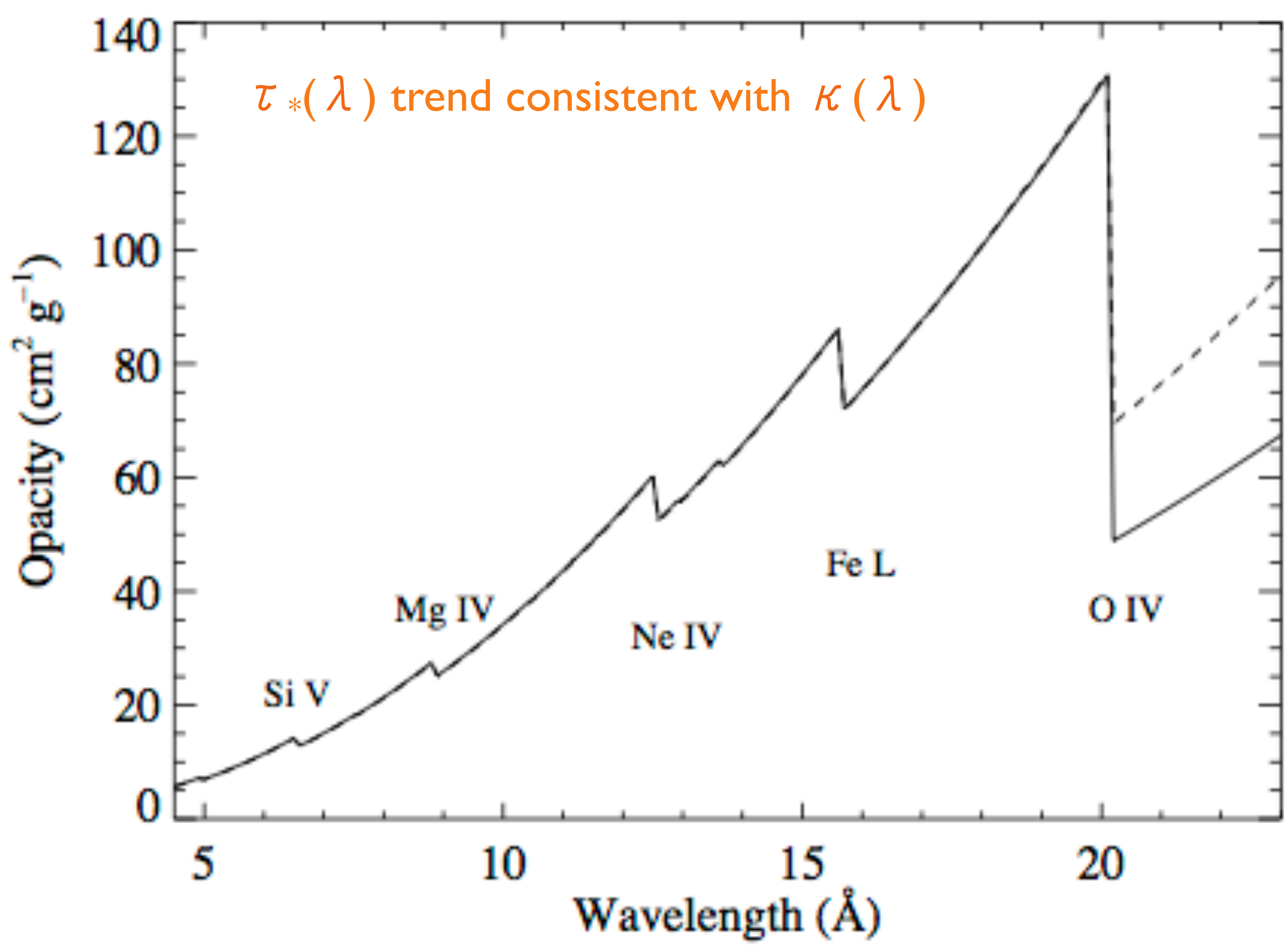

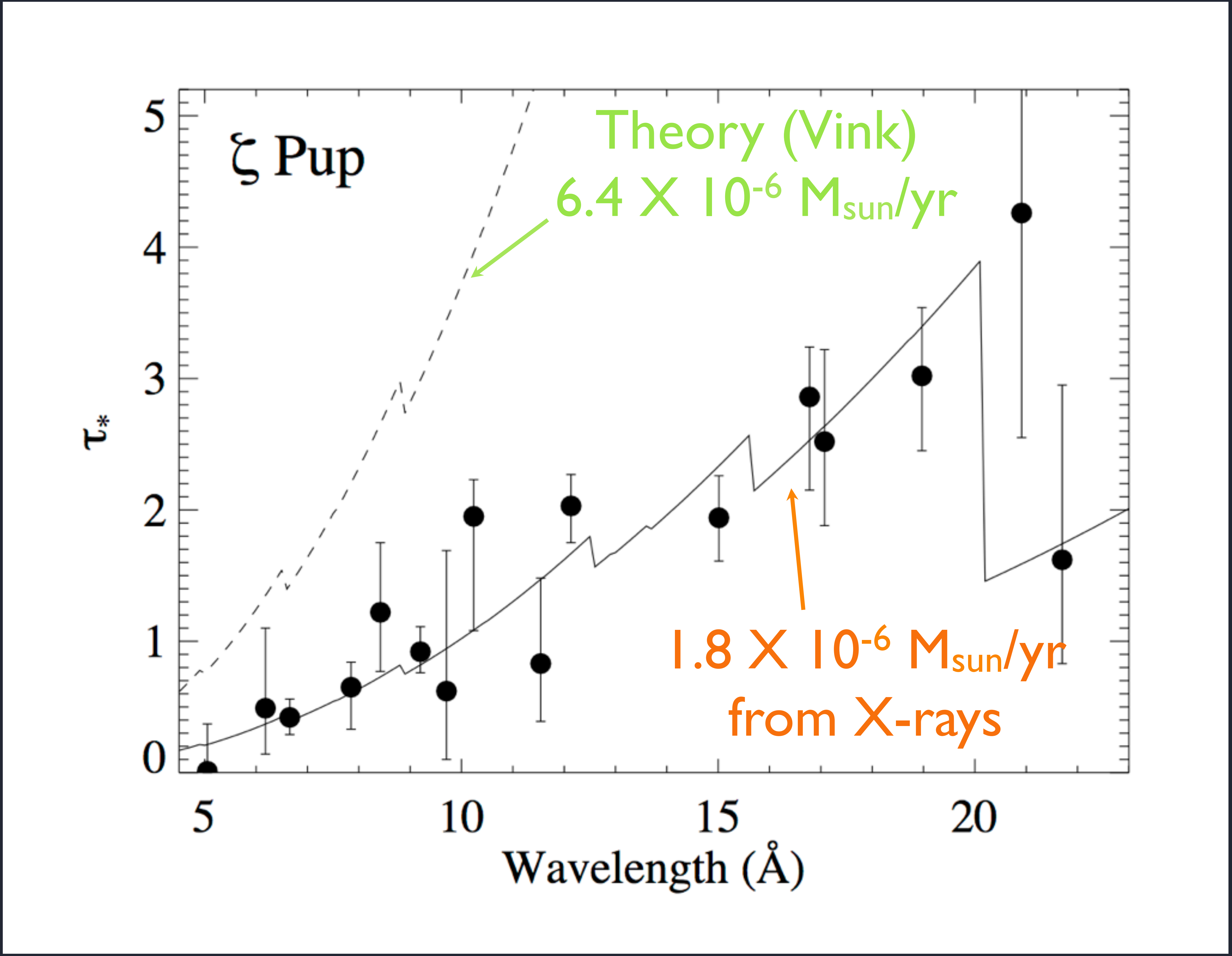

ζ Pup
Theory (Vink)
6.4 X 10-6 Msun/yr
1.8 X 10-6 Msun/yr
from X-rays
τ*
Wavelength (Å)
0
1
2
3
4
5
5
10
15
20

consistent with new UV&IR measurements that model the wind clumping (Bouret et al. 2012, Najarro et al. 2011)

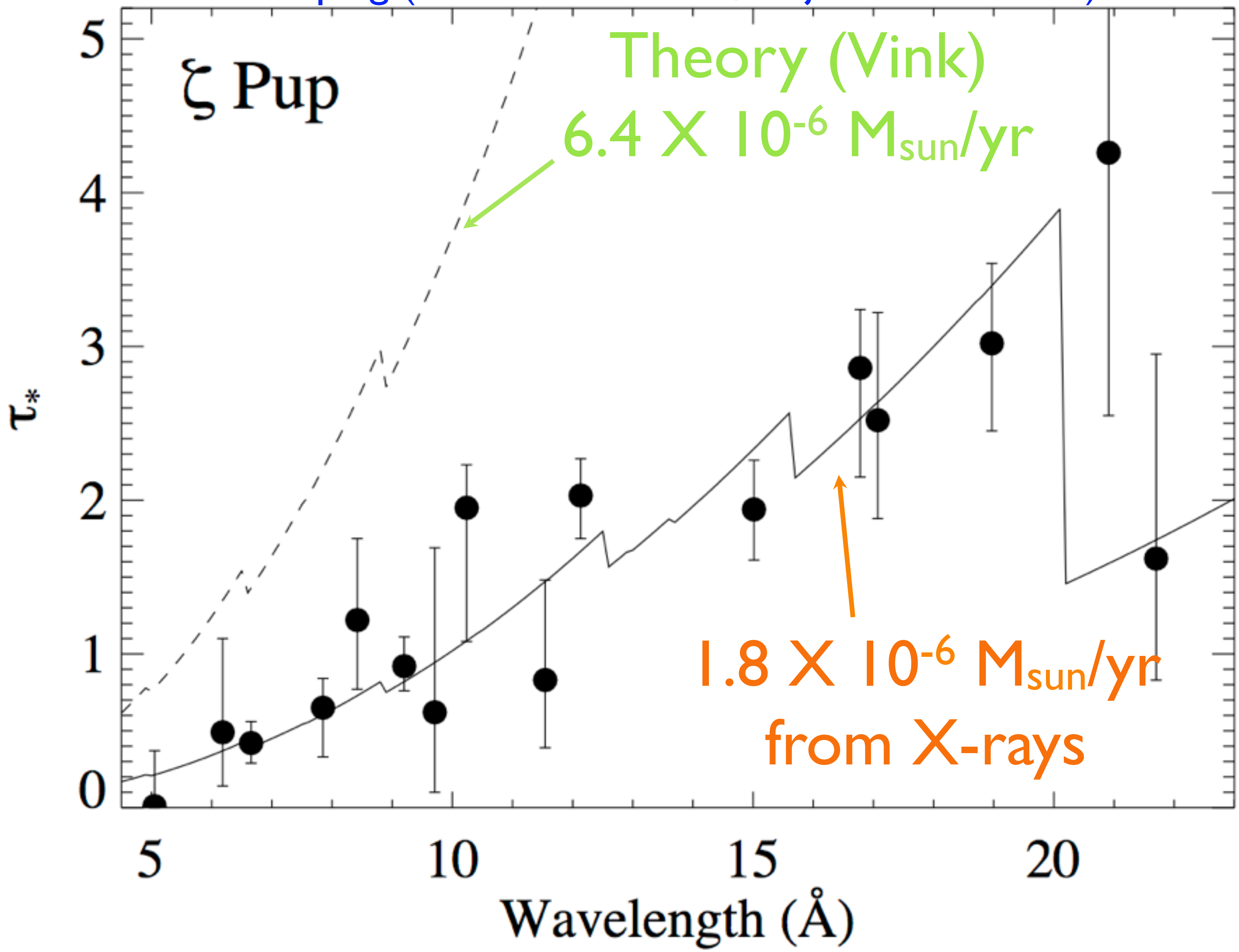

X-ray line profile based mass-loss rate: implications for clumping

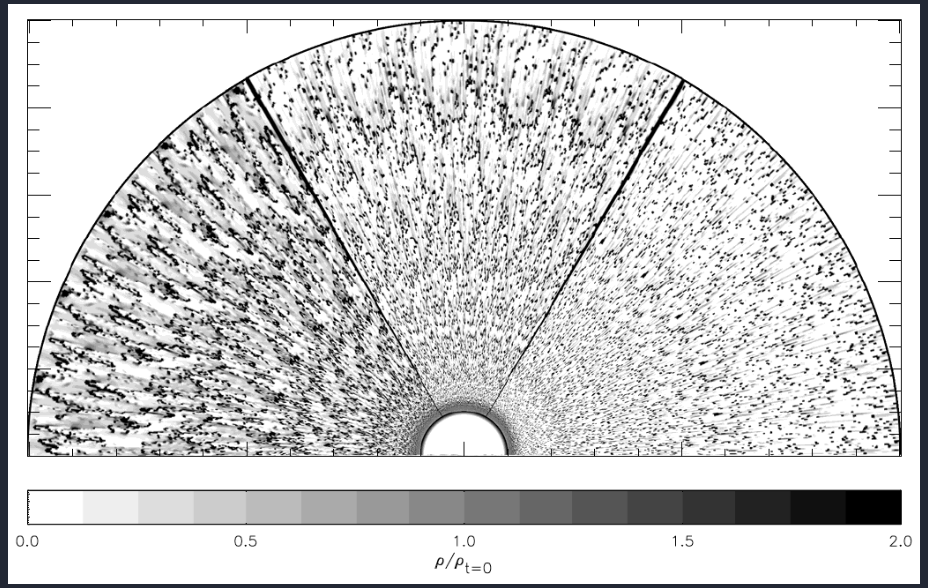

basic definition: $f_{cl} \equiv \langle \rho^2 \rangle / \langle \rho \rangle^2$

clumping factor

ignoring clumping will cause you to *overestimate* the mass-loss rate

but see Oskinova et al. (2007), Owocki (2008), Sundqvist (2010, 2011) - optically thick clumping in the UV

X-ray line profile based mass-loss rate: implications for clumping

basic definition: $f_{cl} \equiv <\rho^2>/<\rho>^2$

clumping factor

from (column) density diagnostic like $\tau_\star$ from X-ray profiles

from density-squared diagnostics like Hα, IR & radio free-free

X-ray line profile based mass-loss rate: implications for clumping

clumping factor $f_{cl} \equiv \langle \dot{M}^2_{H\alpha} \rangle / \langle \dot{M}_{X\text{-ray}} \rangle^2$

$f_{cl} \sim 20$ for ζ Pup

but see Puls et al. 2006, Najarro et al. 2011: radial variation of clumping factor

clumping factor ~10 to ~20 (Najarro et al. 2011)

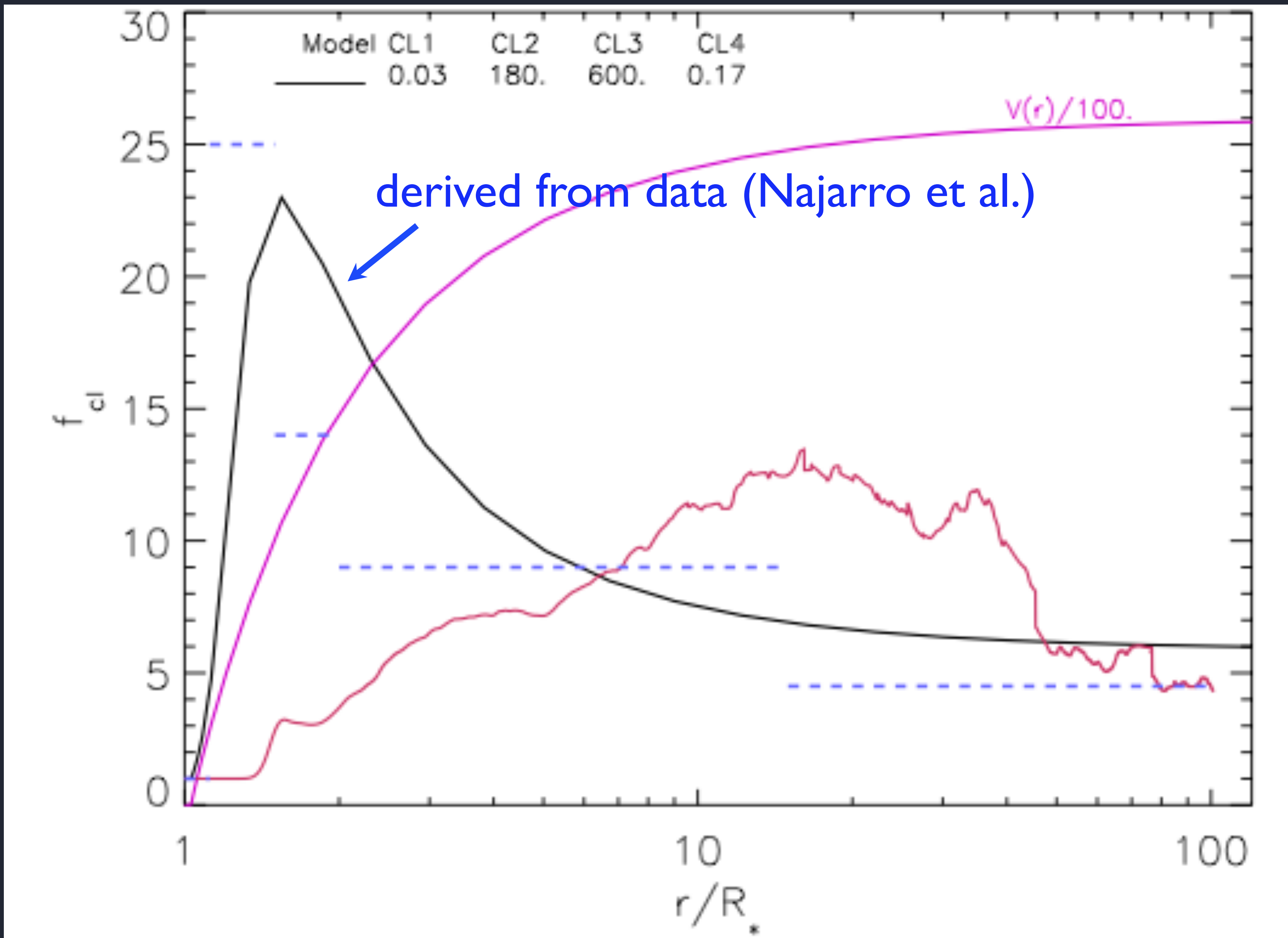

Fig. 18. Radial stratification of the clumping factor, f_{cl}, for ζ Pup. Black solid: clumping law derived from our model fits. Red solid: Theoretical predictions by Runacres & Owocki (2002) from hydrodynamical models, with self-excited line driven instability. Dashed: Average clumping factors derived by Puls et al. (2006) assuming an outer wind matching the theoretical predictions. Magenta solid: run of the velocity field in units of 100 km s^{-1}. See also Sect. 4.

2-D radiation-hydro simulations

clumps break up to the grid scale; $f_{cl} \sim 10$

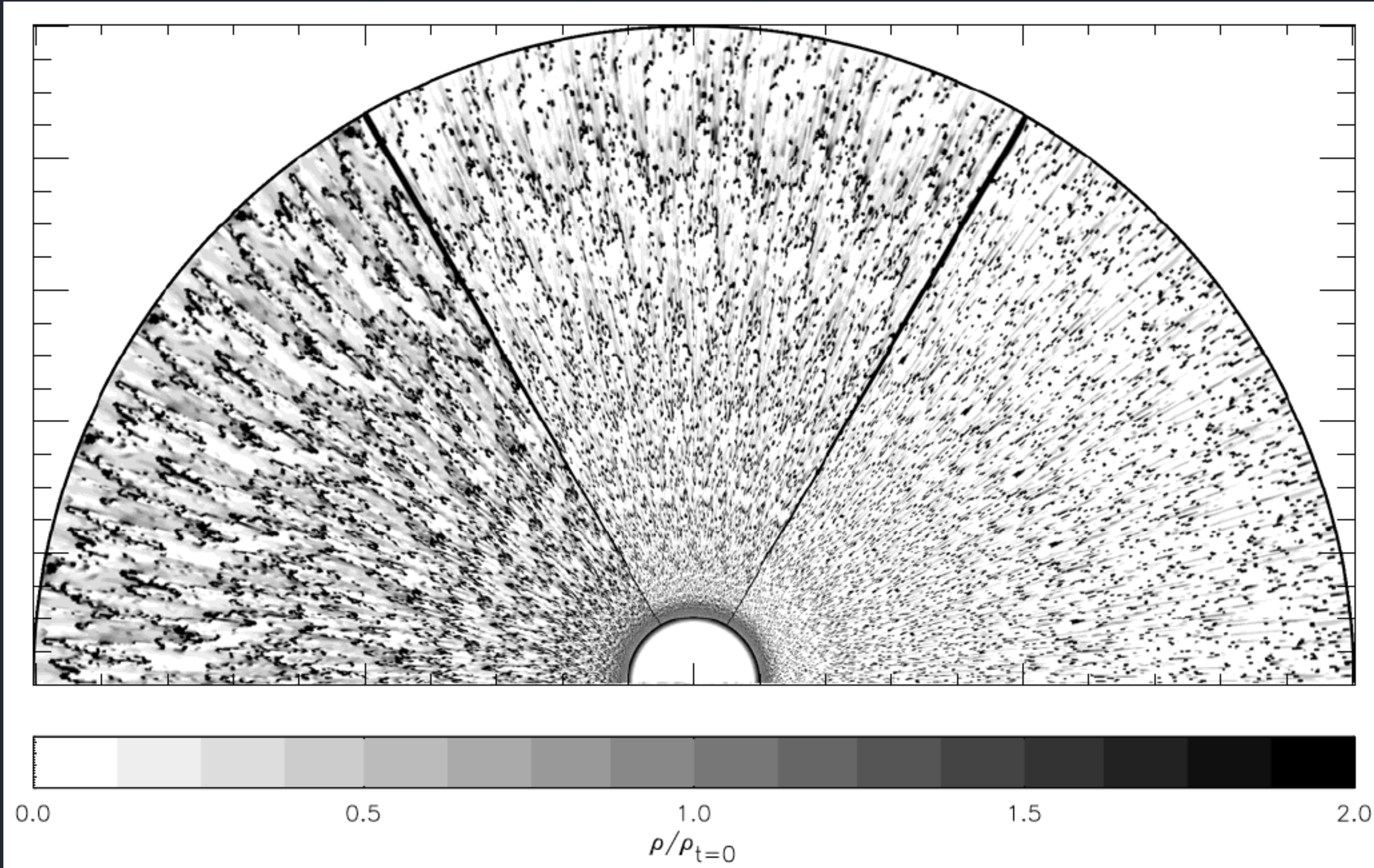

Dessart & Owocki 2003

HD 93129A (O2 If*)

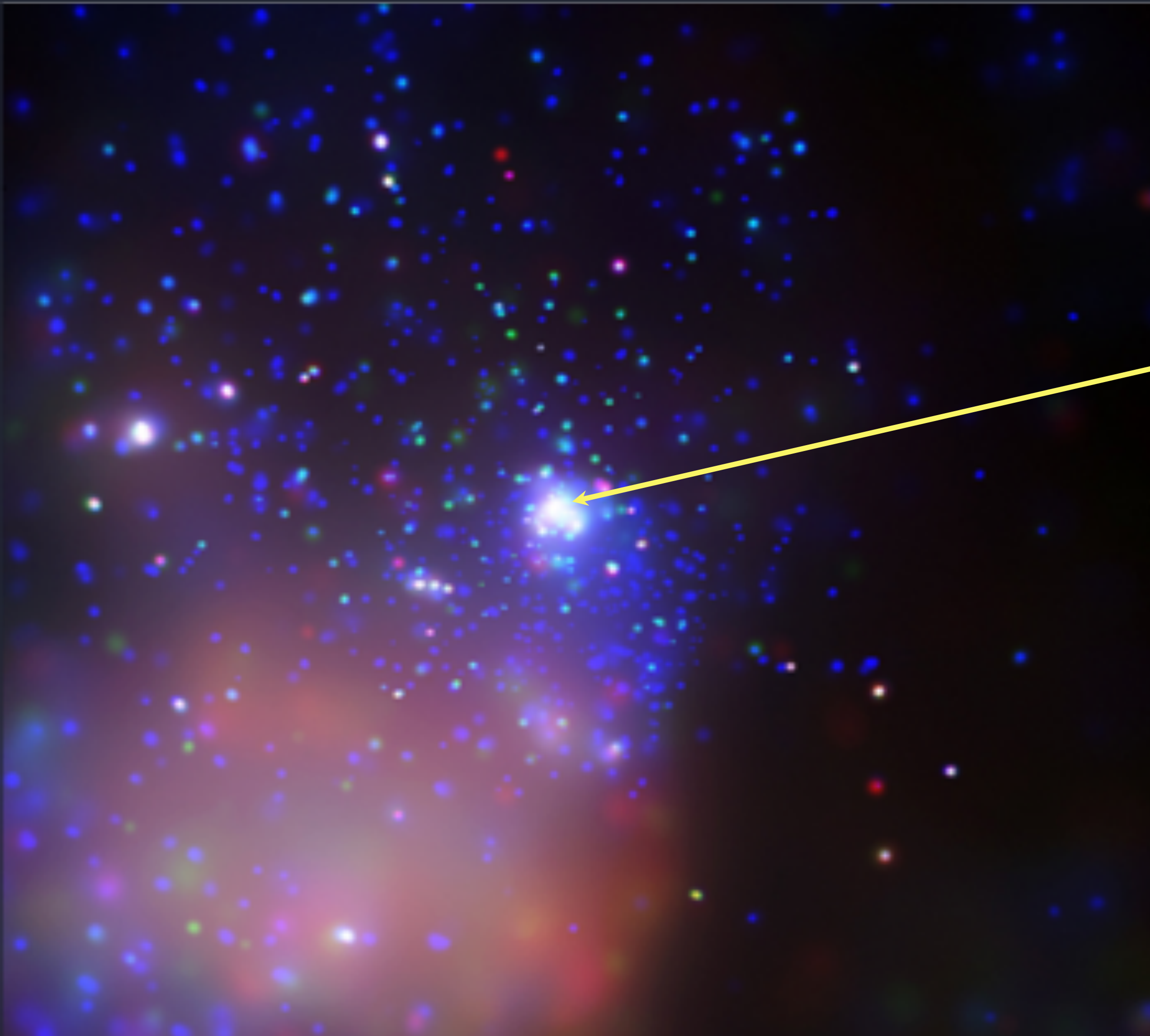

Tr 14: *Chandra*

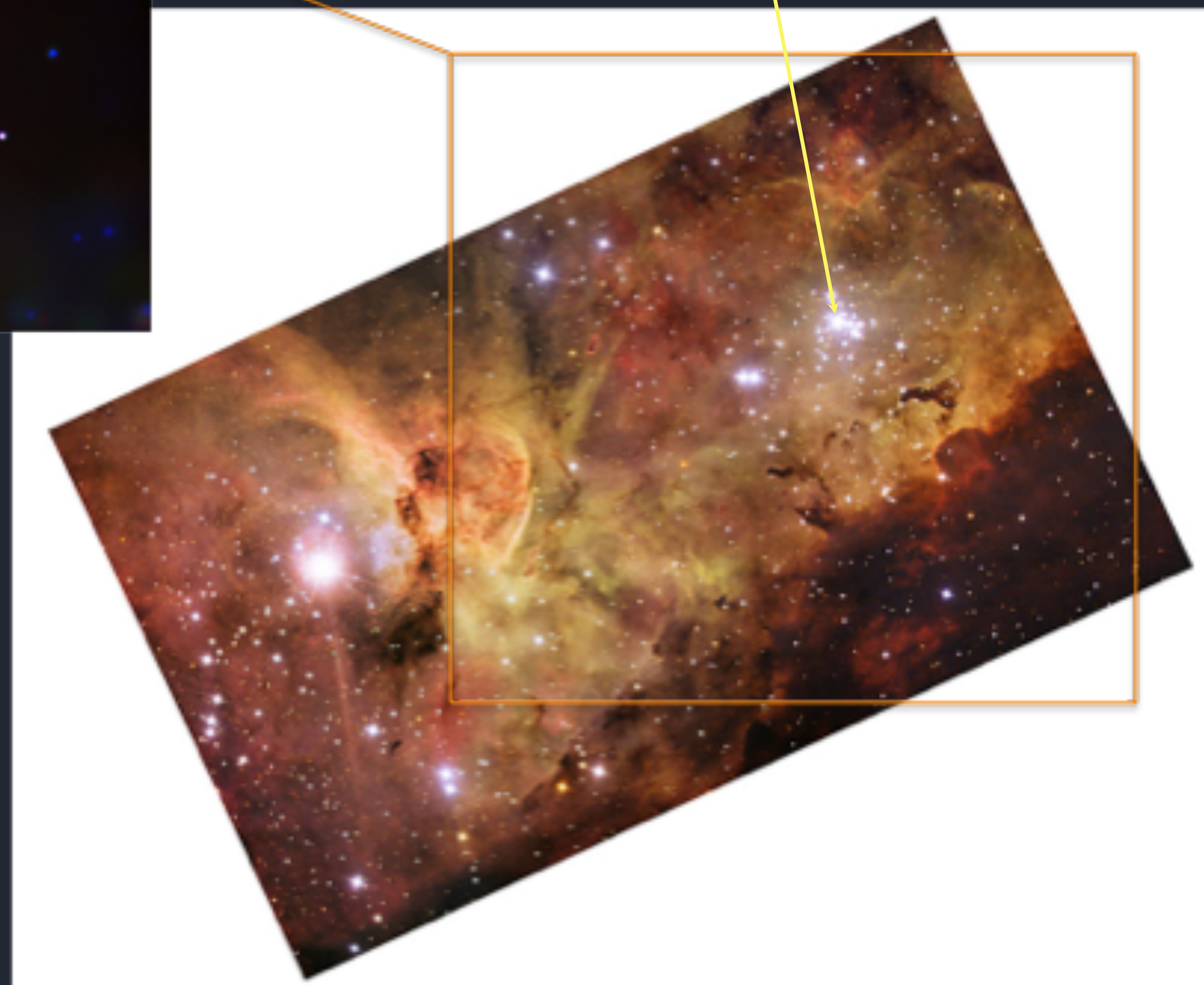

Carina: ESO

Chandra grating spectra of HD 93129A

Cohen et al., 2011, *MNRAS*, 415, 3354

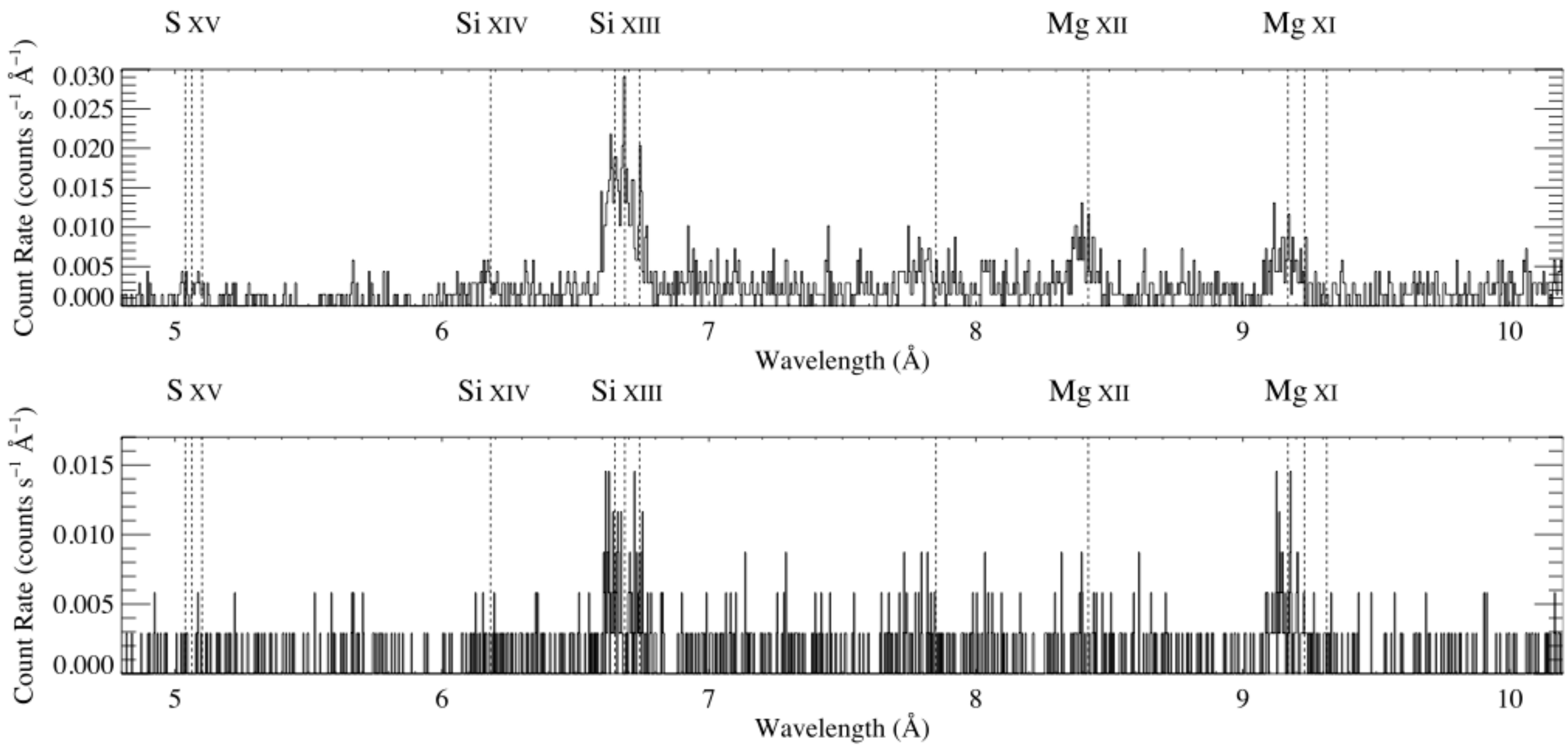

Figure 3. The extracted MEG (top) and HEG (bottom) spectra from the seven coadded pointings. Note the different y-axis scales on the two figures. The wavelengths of lines expected to be present in normal O star *Chandra* spectra are indicated by the vertical dotted lines.

Strong stellar wind: traditional diagnostics

UV

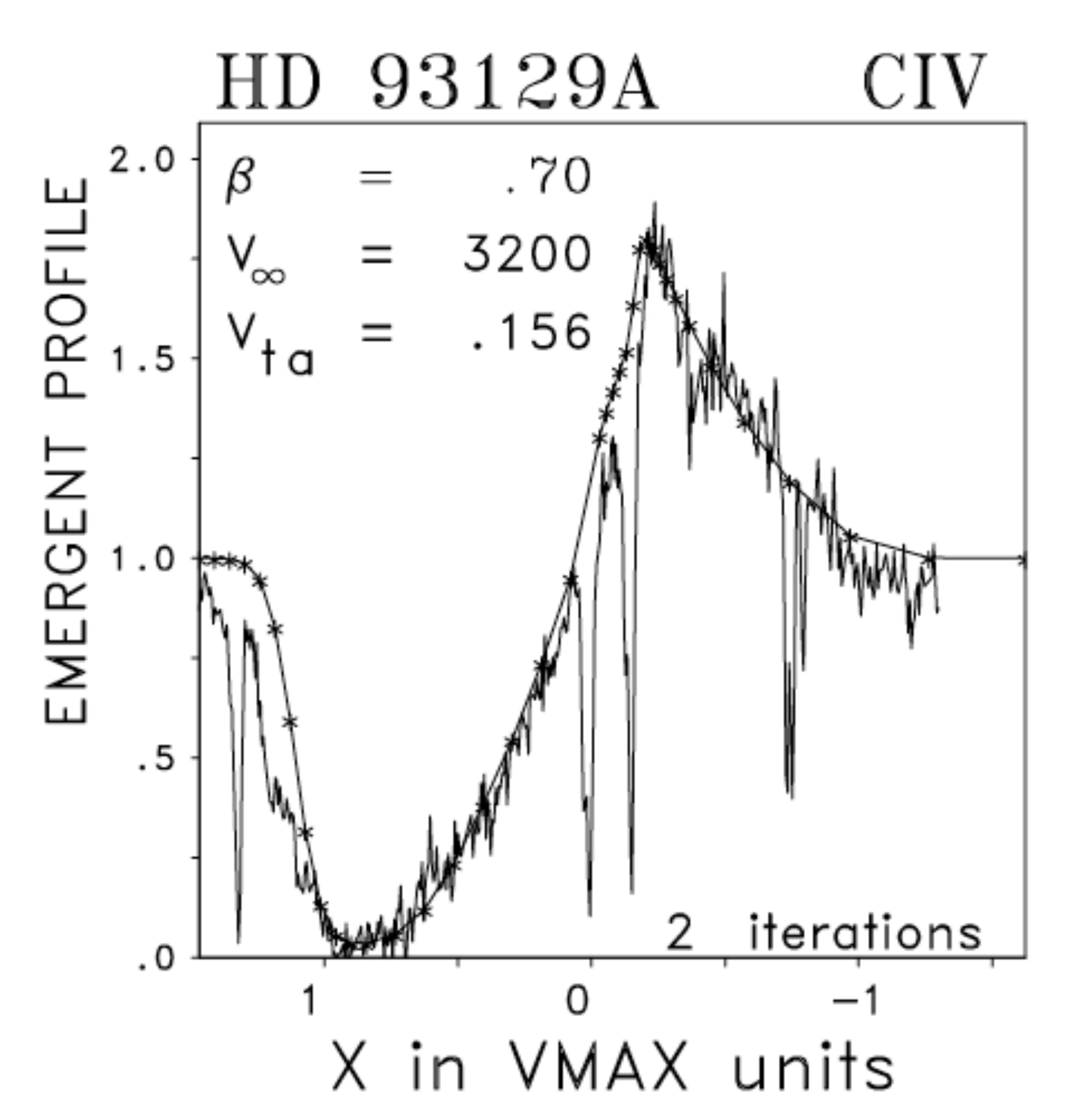

Taresch et al. (1997)

$\dot{M} = 2 \times 10^{-5}\ M_{sun}/yr$

$v_\infty = 3200$ km/s

H α

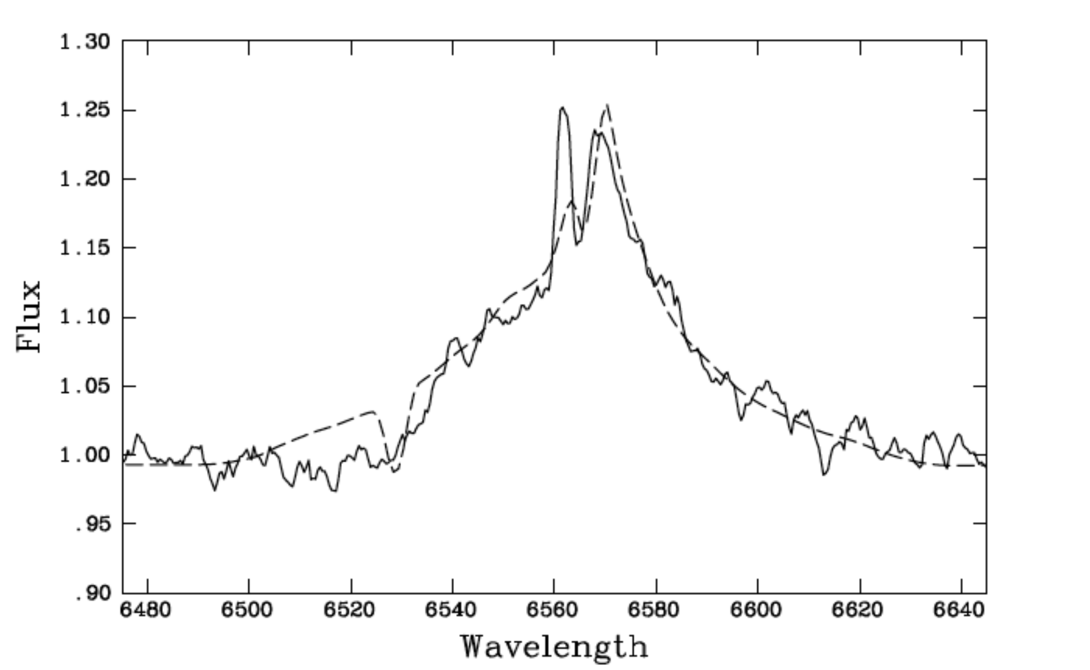

Fig. 13. Observed Hα profile (**solid**) compared with the calculation assuming a mass loss of $18\times10^{-6}\ M_\odot$/yr (dashed). Note that the blue narrow emission peak originates from the H II-region emission.

HD 93129A Mg XII Lyman-alpha

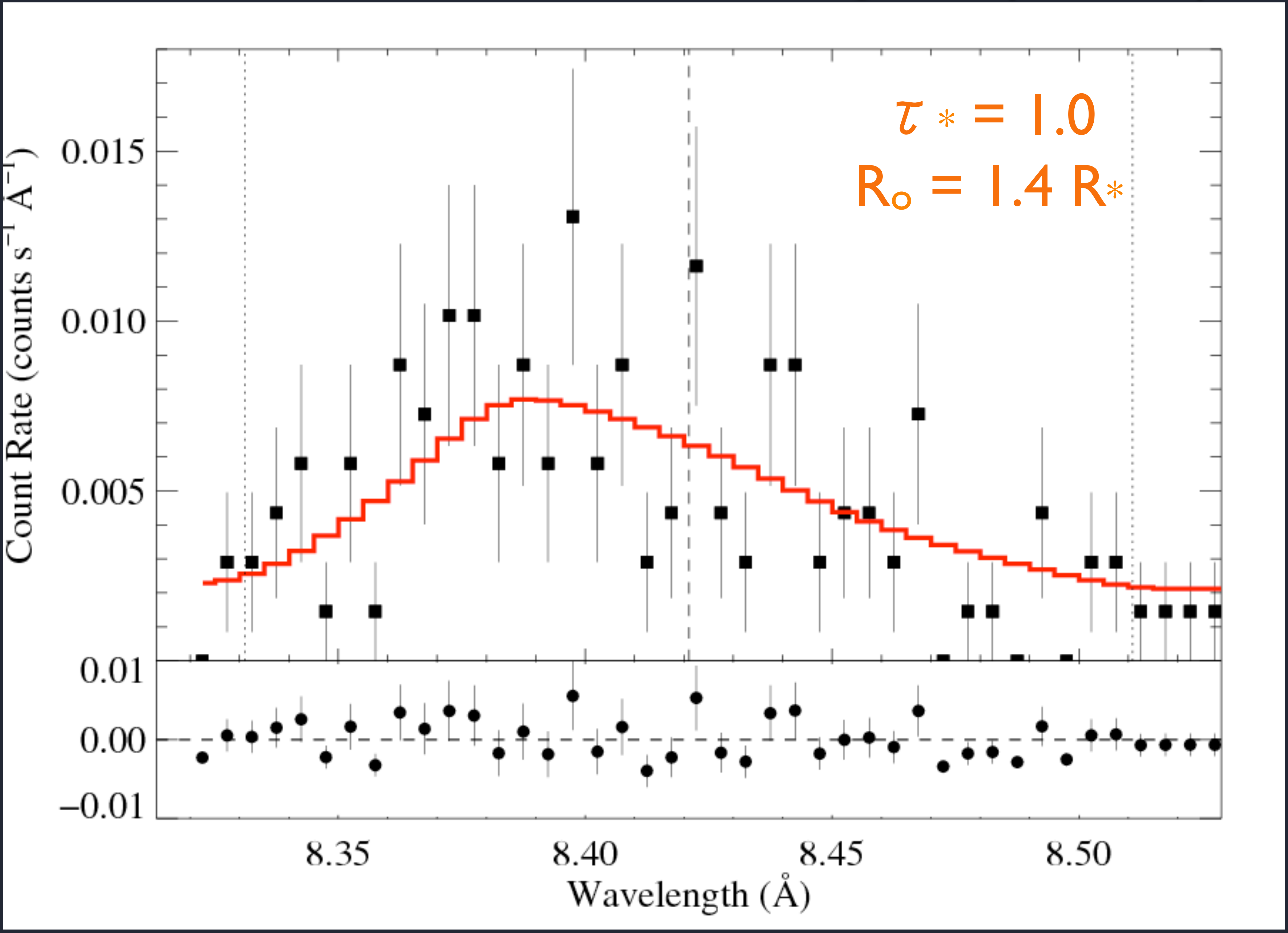

R_o = onset radius of X-ray emission

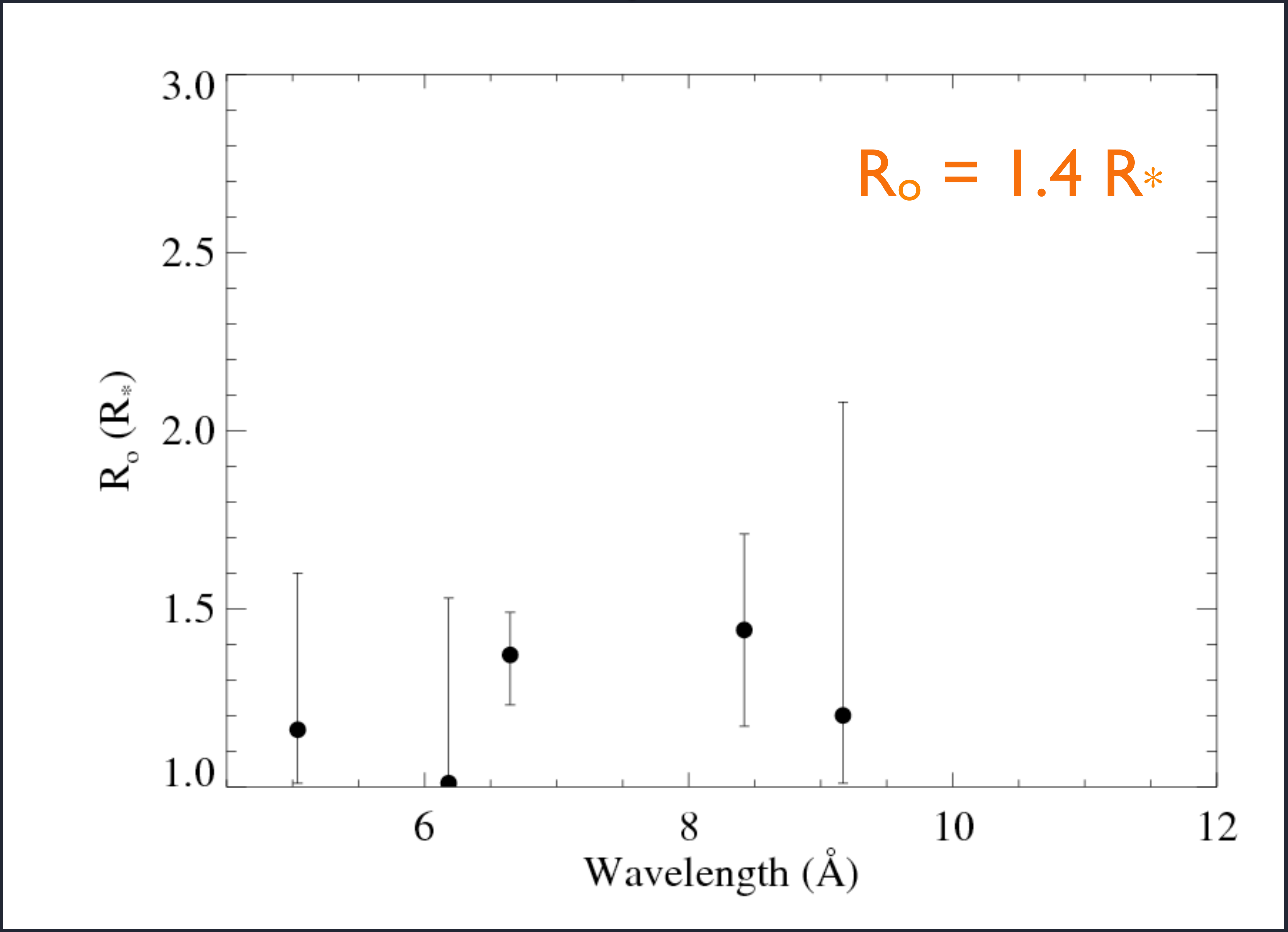

HD 93129A τ_* from five emission lines

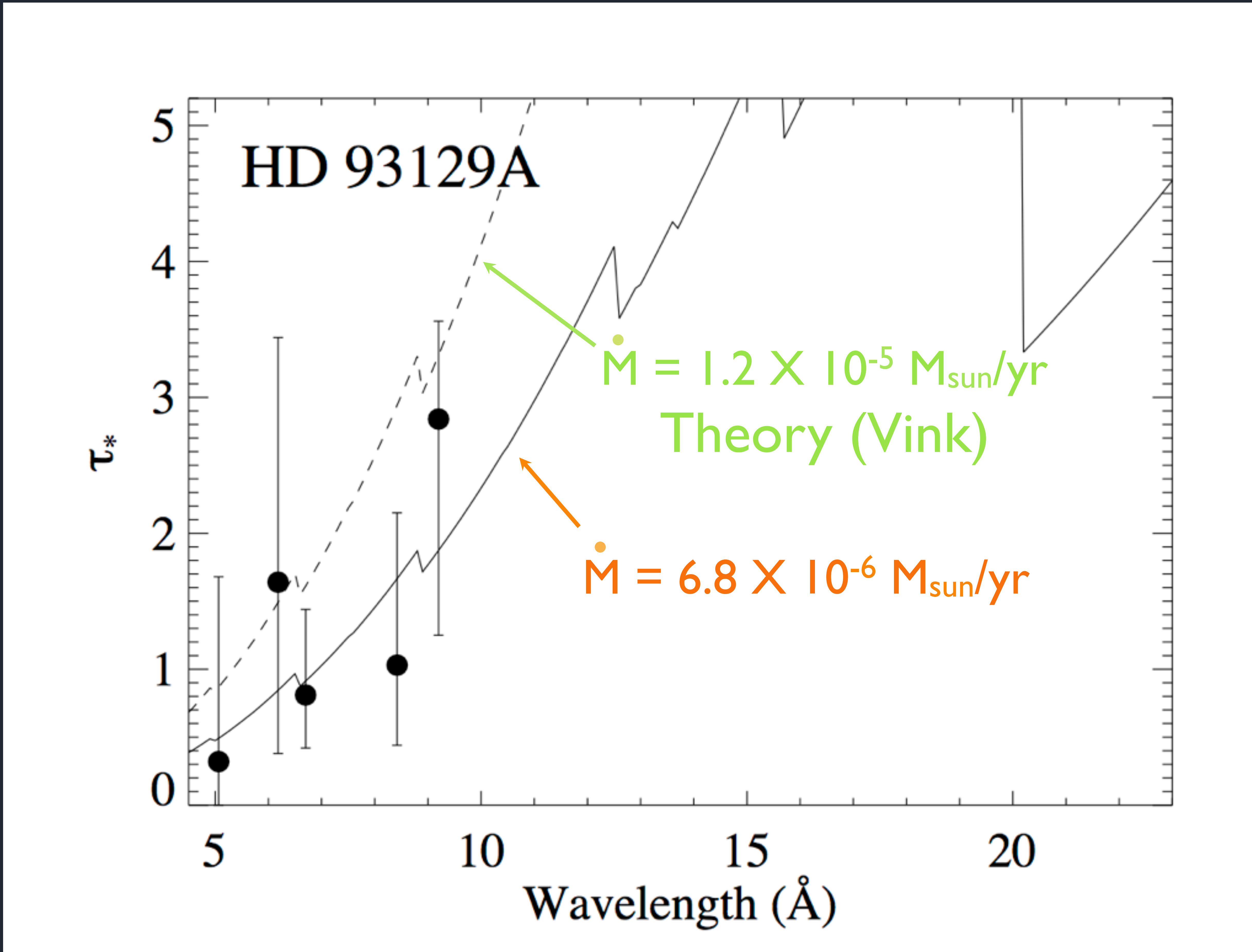

HD 93129A τ_* from *Chandra* ACIS spectrum

using *windtabs* wind absorption model (Leutenegger et al. 2010)

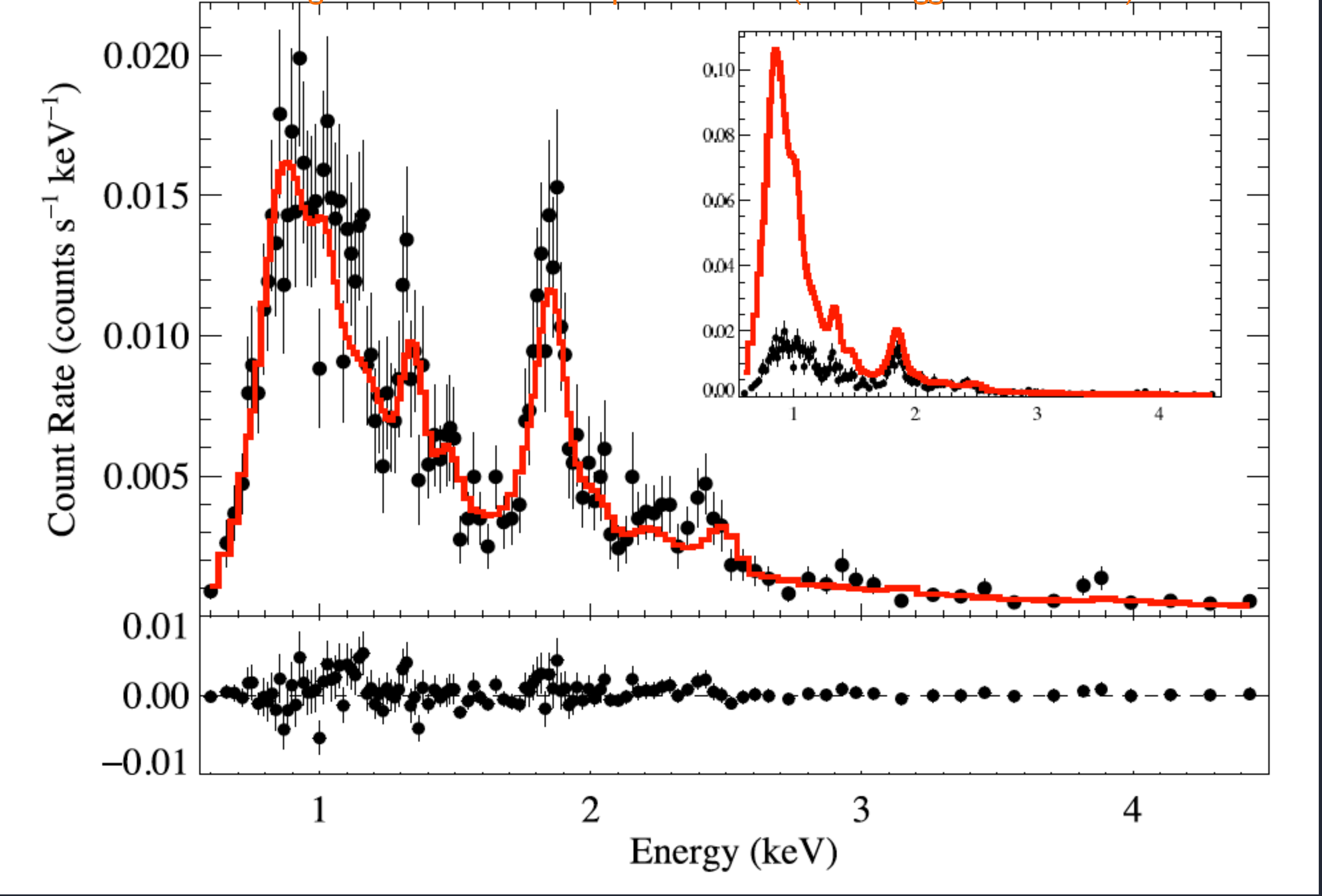

Lower mass-loss rate: consistent with Hα?

Lower mass-loss rate: consistent with H α ?

Yes! With clumping factor of $f_{cl} = 12$

$\dot{M} = 7 \times 10^{-6}\ M_{sun}/yr$

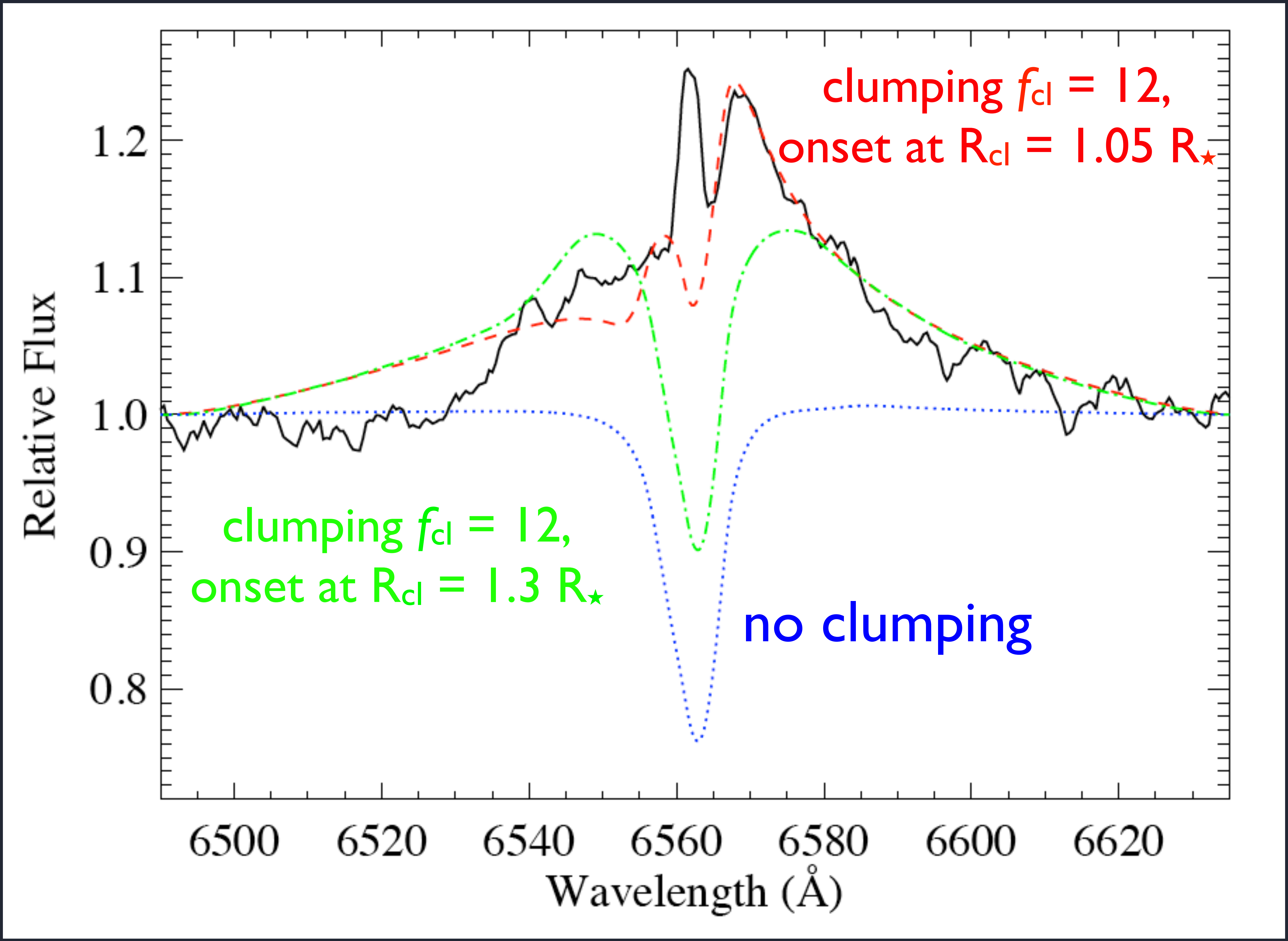

Extension of X-ray profile mass-loss rate diagnostic to other stars

lower mass-loss rates than theory predicts with clumping factors typically of f_{cl} ~ 20

Cohen et al., 2014, *MNRAS*, 439, 908

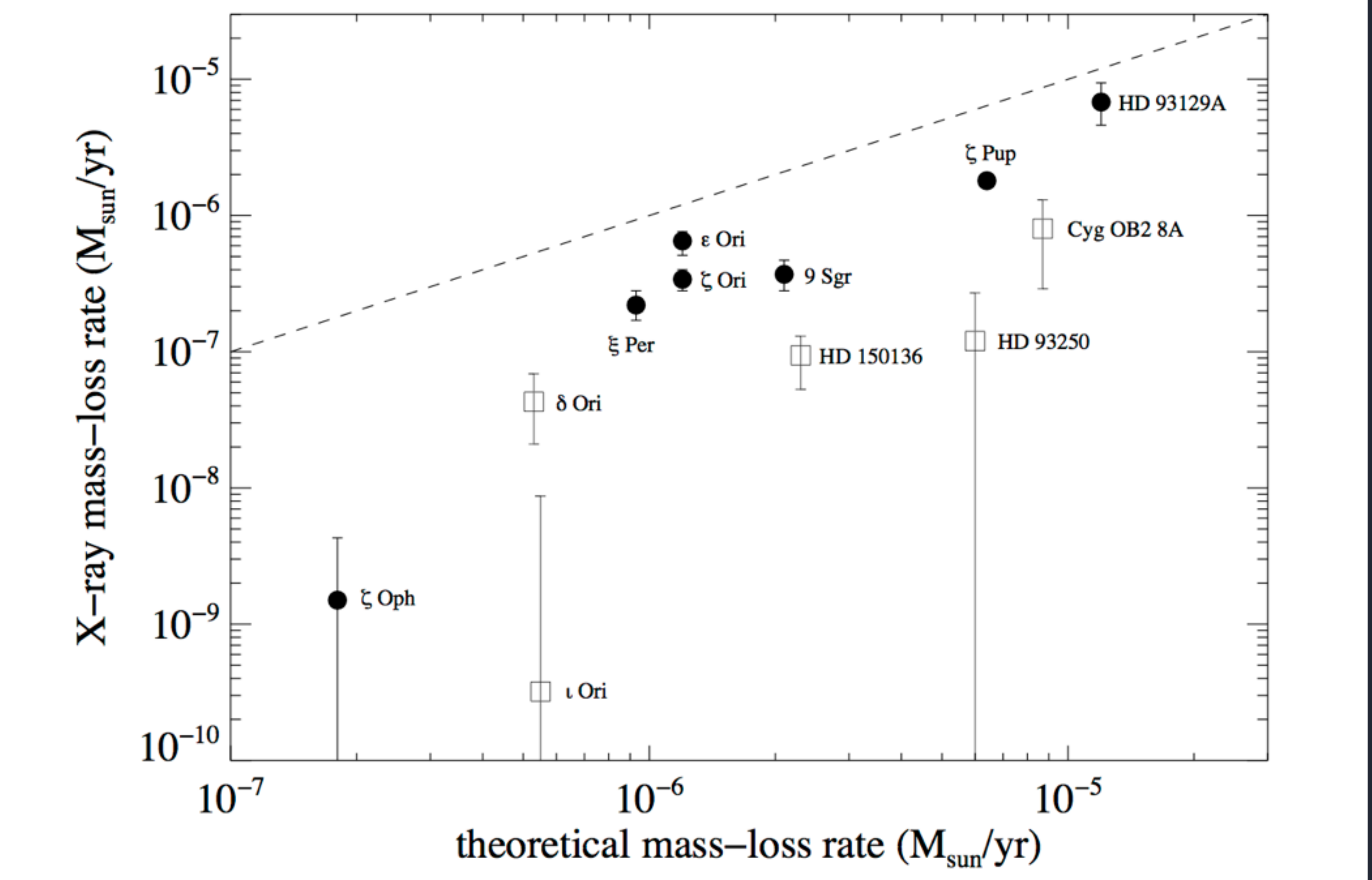

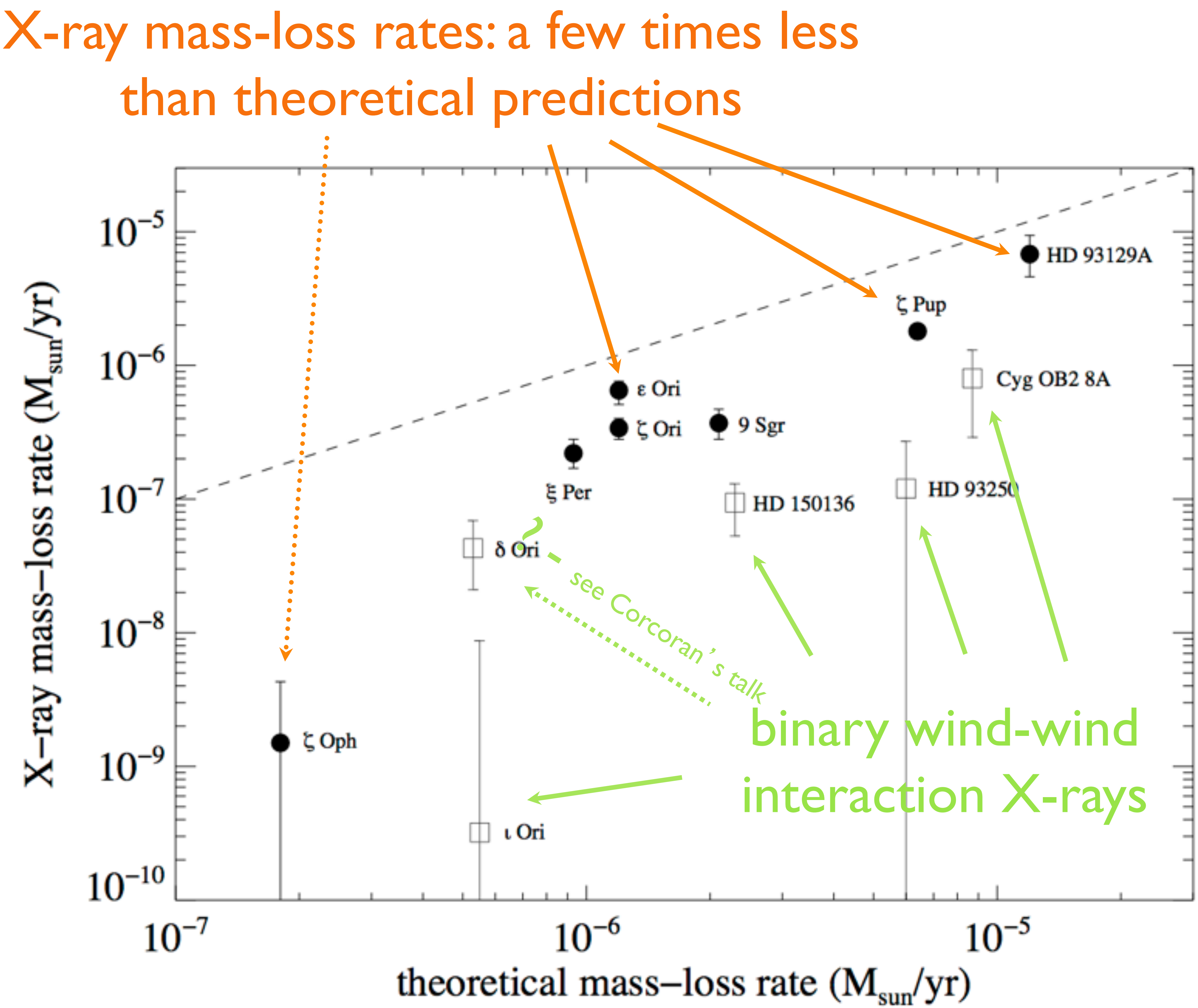
X-ray mass-loss rates: a few times less than theoretical predictions
binary wind-wind interaction X-rays
see Corcoran's talk
X–ray mass–loss rate (M_{sun}/yr)
theoretical mass–loss rate (M_{sun}/yr)
10^{-5}
10^{-6}
10^{-7}
10^{-8}
10^{-9}
10^{-10}
HD 93129A
ζ Pup
Cyg OB2 8A
ε Ori
ζ Ori
9 Sgr
ξ Per
HD 150136
HD 93250
δ Ori
ζ Oph
ι Ori

Conclusions

from *Chandra* resolved X-ray line profile spectroscopy

1. Embedded Wind Shock scenario - inspired by hydro simulations of the LDI - is consistent with X-ray emission properties

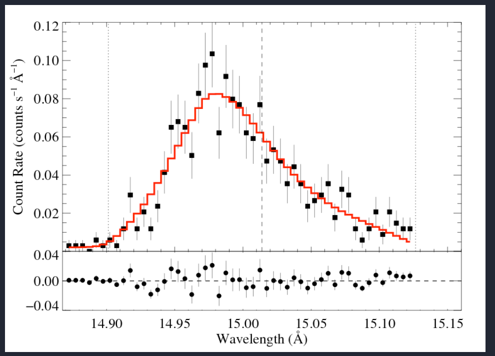

• Mass-loss rates are lowered by roughly a factor of three

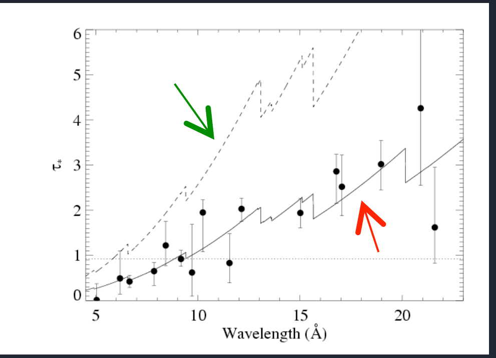

•Clumping factors of order 10 are consistent with optical and X-ray diagnostics

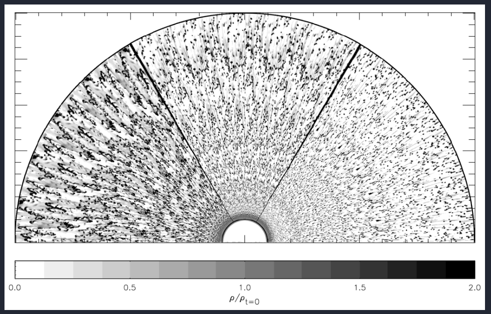

• Clumping starts at the base of the wind, lower than the onset of X-ray emission